Expanding the Geostationary Atmospheric Composition Constellation: Towards Global Coverage

Ali Omar, Emma Knowland, Barry Lefer
NASA

Ana Andries
Surrey University, UK

Paulo Artaxo
University of Sao Paolo, Brazil

Sara Basart
World Meteorological Organization (WMO)

Owen Cooper, **Shobha Kondragunta**
National Oceanic and Atmospheric Administration (NOAA)

Dominika Cyzewska
European Organisation for the Exploitation of Meteorological Satellites (EUMETSAT)

Arlindo daSilva
NASA (retired)

Jonathan E Hickman
NASA GISS (Columbia University)

Sebastian Diez
Universidad del Desarrollo, Chile

Sheldon Drobot, **Dennis Nicks**
BAE Aerospace, USA

Omar Emam
Intospass, UK

Betsy Farris
University of Colorado

James Hannigan, **Pieternel Levelt**, **Shima Shams**, **Helen Worden**
National Center for Atmospheric Research (NCAR)

Eloise Marais
University College of London

Dylan Millet
University of Minnesota, Twin Cities

Ray Nassar, **Christopher Sioris**
Environment and Climate Change Canada (ECCC), Toronto, Canada

Marloes Penning DeVries
University of Twente, Netherlands

Rob Ryan
University of Melbourne, Australia

Raid M Suleiman
Harvard-Smithsonian Astronomical Observatory

Ben Veihelman
European Space Agency (ESA)

Karn Vohra
University of Birmingham, UK

Jun Wang
University of Iowa

Table of Contents

Expanding the Geostationary Atmospheric Composition Constellation: Towards Global Coverage

1. Executive Summary

This white paper proposes a collaborative global framework to expand geostationary (GEO) atmospheric composition monitoring to populated, undermonitored areas facing severe environmental threats. Currently, significant observational gaps exist across Africa, parts of Latin America and the Caribbean, the Pacific Islands, most of Asia (excluding Japan and South Korea), and Oceania (including Australia and New Zealand).

Expanding coverage to these regions is critical due to rapid population growth and urbanization. Future megacities will concentrate populations, intensify environmental pressures, and alter land use. While high-income countries benefit from extensive ground monitoring, this resource is severely lacking in low- and middle-income nations. Without robust monitoring systems, epidemiologists cannot track health impacts, and policymakers lack the real-world observations required to evaluate pollution exposure and develop effective mitigation strategies.

To complement the proposed satellite expansion, this paper also highlights the need to strengthen existing ground-based networks. By identifying coverage gaps, assessing data quality, promoting capacity building, standardizing methodologies, and enforcing quality control, the global community can enable harmonized data utilization for model validation and provide reliable datasets to inform data-based policies in developing countries. This harmonized data will also benefit global air quality models improving the skill of forecast models in developed countries.

GEO satellite data is uniquely suited to fill these monitoring gaps. While Low Earth Orbit (LEO) satellites provide daily global data and ground stations capture high-frequency local conditions, GEO sensors offer a synoptic view of the daytime diurnal cycle. Their hourly measurements capture the rapid atmospheric composition changes driven by shifting emissions, transport, and chemical reactions, comprehensively covering areas between and without ground stations.

This proposed expansion builds upon a highly successful foundation of existing satellite observations, which already form the cornerstone for monitoring air pollution, characterizing emission trends, and improving atmospheric chemistry forecasting. Today, data assimilation successfully combines satellite and ground-based observations with model predictions to produce corrected analyses that feed critical environmental information services.

Presently, the 'GeoAQ Constellation' operates three UV-visible-near infrared spectrometers (GEMS on GEO-Kompsat-2B, TEMPO on Intelsat 40e, and Copernicus Sentinel-4 on MTG-S1) to observe ozone (O_3), nitrogen dioxide (NO_2), formaldehyde (HCHO), and sulfur dioxide (SO_2) (CEOS, 2011, 2019). This white paper proposes to expand the GeoAQ Constellation by strategically adding four geostationary satellites over Africa, South America, the Middle East and India, and Oceania.

2. Introduction

Air quality, determined by the concentration of tropospheric pollutants near the surface, profoundly impacts human health and the global environment. The most critical air pollutants, particulate matter (PM), nitrogen oxides (NOx), sulfur dioxide (SO2), volatile organic compounds (VOCs), ozone (O3), ammonia (NH3), carbon monoxide (CO), and lead (Pb), originate from a complex mix of natural and anthropogenic sources. PM is a heterogeneous mixture of organic compounds, sulfates, nitrates, metals, black carbon, and biological materials that forms directly from combustion and mechanical processes, or secondarily through atmospheric reactions. Anthropogenic emissions, such as NOx from high-temperature fuel combustion, SO2 from sulfur-containing fuels, VOCs from industrial and household activities, and NH3 from agriculture, combine with natural emissions like biogenic VOCs from vegetation, volcanic SO_2, and NOx from soils and lightning. Together, these precursors drive the photochemical formation of secondary pollutants like O_3, while CO serves as a primary indicator of incomplete combustion from biomass burning.

While developed nations have successfully reduced pollutants through strict regulations (**https://gispub.epa.gov/air/trendsreport/2024/#welcome**), and countries like China have seen significant drops over the last decade (Science, 2026), pollution from natural and anthropogenic sources still dominates much of the world. In India, for example, winter smog is severely exacerbated by crop residue burning combined with trapped urban emissions (Kajino et al., 2025; Kaskaoutis et al., 2014). In the Southern Hemisphere, Africa and Southeast Asia experience consistent seasonal fires and dust, whereas South American and Australian wildfires are extreme and episodic. The rapid emergence of megacities in these Southern regions urgently warrants continuous monitoring and policy development.

To address this global pollution grand challenge, the science of atmospheric composition monitoring has matured significantly. Space-based observation evolved from Low Earth Orbit (LEO) instruments like GOME and SCIAMACHY, which required several days for global coverage, to the high-resolution, daily capabilities of modern sensors. Historical milestones include the Tropospheric Ozone Residual method, which pioneered satellite-based ozone quantification from 1979 to 2005 (Gaudel et al., 2018), and GOME's profile retrievals, which, combined with OMI, created near-continuous O_3 records (Gaudel et al., 2018). NASA further advanced the field by combining OMI and MLS data via assimilation (Ziemke et al., 2011).

Today, Sentinel-5P TROPOMI is revolutionizing air quality monitoring. Its tropospheric NO_2 retrievals are widely used for emissions tracking and forecast improvement (**https://atmosphere.copernicus.eu/**), as well as assessing impacts like the COVID-19 lockdowns (Levelt et al., 2022). Furthermore, thermal infrared (TIR) observations from IASI and CrIS have enabled the measurement of NH_3 (Cao et al., 2022; Whitburn et al., 2016), peroxyacetyl nitrate (Payne et al., 2022), isoprene (Wells et al., 2020), and other VOCs (Franco et al., 2022; Wells et al., 2025).

Historically, the CEOS Atmospheric Composition Virtual Constellation (AC-VC) relied on LEO missions for daily global observations, leaving a glaring gap in our ability to observe pollutants diurnally. Geostationary (GEO) instruments like GEMS, TEMPO, and Sentinel-4 (which adds NH_3, CO, and IR-absorbing VOC capabilities) now fill this gap, capturing diurnal variations driven by time-dependent emissions like rush-hour traffic and daytime photochemistry. However, the current GeoAQ Constellation only covers the Northern Hemisphere where air quality policies are already mature (Millet et al., 2024), underscoring the need for an expanded GeoAQ Constellation capable of continuous, diurnally resolved global coverage.

Moving forward, LEO and GEO capabilities will operate in synergy. The LEO follow-on to TROPOMI, Sentinel-5/UVNS, launched in August 2025. Orbiting beneath the GeoAQ Constellation, Sentinel-5 and Sentinel-5P measure at 9:30 AM and 1:30 PM respectively, serving as vital transfer standards for cross-calibrating GEO sensors at different times. As a second generation of GeoAQ Constellation sensors approaches, synergistic retrievals combining imagers and spectrometers will become the norm. For example, using VIIRS to inform TROPOMI methane algorithms about cloud cover enhances the derived air quality data.

Additionally, fusing TIR and UV/VIS observations greatly improves retrieval sensitivity in the lower troposphere. Studies have shown that combining IASI and GOME-2 increases the degrees of freedom for lowermost tropospheric ozone detection (Cuesta et al., 2013), while multispectral synergy enhances the detection of boundary layer pollution (Fu et al., 2018). MOPITT also utilizes this combination, merging TIR profile data with near-infrared column information to boost sensitivity to near-surface CO, particularly in areas with low thermal contrast (Worden et al., 2010). Ultimately, this integrated constellation of LEO and GEO sensors supports a host of advanced applications, from deriving hourly top-down anthropogenic emissions to real-time hazards monitoring and species-specific exposure studies.

3. The Consequence: Where Measurement Gaps Exist and Their Impact

In the Northern Hemisphere, geostationary satellites (Figure 1) have unequivocally proven the transformative value of continuous, high-temporal-resolution atmospheric monitoring. Transitioning from daily to hourly surface PM2.5 estimates, such as those derived from the GOES Advanced Baseline Imager (Zhang et al., 2022), has revolutionized air quality nowcasting, providing alerts that could save an average of 1,200 lives and $13 billion in healthcare costs annually (O'Dell et al., 2024).

High-resolution NO2 observations from instruments like TEMPO effectively capture complex diurnal cycles driven by morning traffic, industrial activity, and boundary layer dynamics (Fioletov et al., 2025; Nawaz et al., 2025; Zhang et al., 2025). These continuous daytime scans allow for unprecedented spatial fidelity in estimating hourly NOx emissions (Sun et al., 2025) and reveal critical shifts in metropolitan ozone production, which frequently moves from NOx-saturated regimes in the morning to NOx-limited regimes in the afternoon (Jin et al., 2025). Assimilating this hourly NO2 data into chemical transport models demonstrably reduces biases in emission inventories and improves regional ozone forecasting (Hsu et al., 2026). Furthermore, the data is robust enough to capture sharp gradients over challenging wintertime snowscapes when proper corrections are applied (Griffin et al., 2026), and has proven vital for identifying highly polluted, localized hotspots that currently lack ground sensors (Siu et al., 2025).

Beyond NO2, TEMPO expands our monitoring capabilities to track the diurnal variability of formaldehyde (HCHO), though continuous ground-based validation remains necessary (Ortega et al., 2026), and provides high-cadence SO2 measurements for the rapid hazard mitigation of anthropogenic and volcanic plumes (Li et al., 2025). Maximizing these capabilities, however, requires rigorous calibration; studies evaluating TEMPO and TROPOMI alongside WRF-Chem models highlight that failing to account for cloudy conditions leads to systematic underestimations of NO2 (Goldberg et al., 2025).

Despite these remarkable advances in the Northern Hemisphere, severe observational gaps persist in the Southern Hemisphere (SH). Currently, there are no geostationary UV/VIS satellites capable of measuring the diurnal cycles of NO_2, SO_2, VOCs, and aerosol optical depth (AOD) over highly populated regions outside the USA, Europe, and parts of Asia. For example, Low Earth Orbit (LEO) satellites, even with three VIIRS instruments available, cannot capture the full diurnal variation of smoke from Amazonian fires. This blind spot is alarming given the unprecedented population growth in the SH, a severe lack of ground-based measurements, and the expectation that global emissions will increasingly shift southward.

This geographic gap is compounded by technological and instrumental limitations over the global South. Existing geostationary infrared (IR) sounders like IRS (covering Africa), IASI, and CrIS were built primarily for meteorology, meaning their air quality products are not an operational priority. While they suffer from limited near-surface sensitivity (Clerbaux et al., 2009), making these products an operational priority would vastly improve our understanding of NH3, isoprene, and CO over Africa. There is still some work to do in exploring the capabilities and optimal retrieval strategies of geostationary sounders like MTG IRS and GIIRS-2 (Liang et al., 2024; Sheng et al., 2025; Zeng et al., 2024), especially given the algorithmic discrepancies between LEO and GEO platforms and the vertically dependent sensitivity of thermal IR sounders to VOCs and ammonia.

The current GeoAQ Constellation missions lack co-located carbon monoxide (CO) measurements alongside precursor gases. CO is a vital indicator of incomplete combustion and a major precursor to ozone formation (Seinfeld & Pandis, 2016). Without simultaneous CO observations, scientists cannot easily disentangle the complex chemical processes driving air pollution episodes, accurately attribute pollution sources, or evaluate the effectiveness of emission control measures. While IASI and IRS can be used to track pollution transport, fully addressing this gap would require adding SWIR instrumentation or a MOPITT-type sensor, especially since the GeoCARB mission, which was designed to measure CO2, CH4, and CO from geostationary orbit, was ultimately canceled (Polonsky et al., 2014). While noting their importance, CO and greenhouse gases are beyond the scope of this white paper.

4. The GeoAQ Constellation and the Geostationary Advantage

Geostationary (GEO) satellites offer a transformative approach to Earth observation, fundamentally changing how we monitor the atmosphere by providing continuous, real-time surveillance of targeted regions. Positioned at an altitude of 35,786 kilometers, these satellites orbit at the exact rate of the Earth's rotation. This unique vantage point allows them to hover over a single geographic location, capturing new imagery every 5 to 15 minutes. Rather than relying on fleeting glimpses, GEO platforms watch atmospheric chemistry, pollution events, and weather systems dynamically unfold throughout the day.

The continuous monitoring capability of TEMPO, Sentinel-4 and GEMS satellites (Figure 1), becomes indispensable when studying transient atmospheric events that evolve over hours rather than days. For example, the diurnal cycle of urban air pollution is highly dynamic, fluctuating rapidly with shifting traffic emissions, sunlight-driven photochemical reactions, and boundary layer changes. A LEO satellite might capture a clean morning snapshot and a polluted afternoon snapshot, but it completely misses the gradual accumulation, the midday intensification, and the evening decline. GEO satellites, conversely, reveal the complete lifecycle of these pollutants. Furthermore, this high-frequency temporal advantage is vital for detecting and responding to sudden environmental disasters, such as volcanic eruptions, industrial accidents, or power plant malfunctions. If an emission event occurs shortly after a LEO satellite passes overhead, it might remain undetected for over 12 hours, by which time the hazardous plume could have dispersed beyond recognition or traveled hundreds of kilometers. GEO satellites capture these emergencies the moment they happen, tracking the movement, spread, and dilution of plumes hour by hour to inform critical air quality, emergency response, and aviation safety decisions.

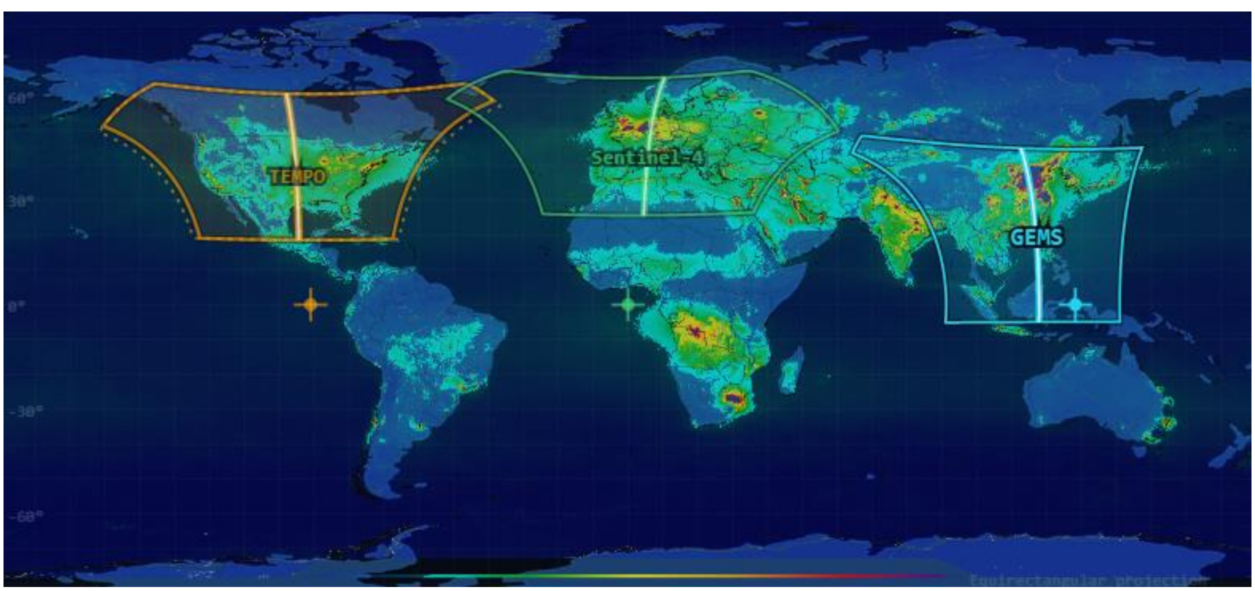

Figure 1. The current "GeoAQ Constellation" of geostationary air quality satellites overlaid on a map of global tropospheric NO_2 concentrations. This foundational constellation comprises TEMPO over North

America, Sentinel-4 over Europe, and GEMS over East Asia. Together, these instruments provide unprecedented continuous, hourly daytime monitoring of short-lived pollutants and their diurnal cycles. However, as the map illustrates, their fields of regard are largely confined to the Northern Hemisphere, leaving polluted regions in Africa, South America, Middle East and India, and Oceania.

5. Evaluating Orbital Architectures: The Case for an Expanded GEO Constellation in Global Air Quality Monitoring

When designing a global air pollution monitoring system, LEO constellations initially seem attractive due to their proximity to the Earth, typically operating between 400 and 800 kilometers. This lower altitude affords LEO satellites superior spatial resolution to observe highly localized emission sources and the ability to achieve truly global coverage, sweeping over the high latitudes and polar regions that other GEO orbits, with the exception of the inclined GEO orbits, inherently miss. However, the critical flaw for air pollution studies of LEO architecture lies in its poor temporal resolution. Air quality is highly dynamic, fluctuating wildly with weather patterns, sunlight, and rush-hour traffic, yet a reasonably sized LEO constellation of 4 LEOs can only capture isolated snapshots of a specific location each day.

Conversely, GEO satellites, stationed at roughly 35,786 kilometers, offer an observational paradigm that perfectly aligns with the fleeting, fast-moving nature of atmospheric pollutants. While their extreme distance requires larger optics for high spatial resolution and results in a complete blind spot over the poles, GEO satellites compensate by providing a continuous, staring gaze over specific regions. This allows a GEO network to deliver the hourly or sub-hourly temporal resolution necessary to track the entire diurnal life-cycle of pollution, from morning industrial emissions to afternoon photochemical ozone formation and unexpected wildfire plumes. Because the vast majority of the human population lives outside the polar zones, capturing these rapid, real-time atmospheric shifts over major continental landmasses is vastly more critical for actionable public health forecasting than the static, a few times-a-day snapshots provided by a reasonably sized LEO network.

Weighing these trade-offs, a dedicated constellation of four new GEO satellites emerges as the superior and recommended architecture. Such a configuration creates a highly robust, strategically overlapping system (*cf.* Figure 2). This overlap optimizes viewing angles to reduce data distortion at the edges of each satellite's footprint, ensures uninterrupted monitoring of pollution transport, and localizes the risk of a single-point hardware failure to a single region. This white paper assumes that there will be a few polar-orbiting LEO satellites operating in conjunction with the expanded GEO constellation providing complementary measurements especially at the poles where the LEO orbit tracks are dense and the repeat cycle is only a few hours. Additionaly, an inclined geostationary orbit dedicated to the high latitude regime may be the most efficient way to observe this region.

6. Closing the Observational Gap: The Public Health Imperative for a Global Geo-Belt

To visualize this comprehensive global solution, Figure 2 maps the complete, expanded geostationary constellation over a global composite of tropospheric NO_2 concentrations. The foundational GeoAQ Constellation, comprising TEMPO, Sentinel-4, and GEMS, is expanded by integrating four additional dedicated platforms into this network: Geo SA (South America), Geo S (Africa), MEASMA Geo N (Middle East and India), and Geo OCN (Oceania), to effectively close these geographic blind spots.

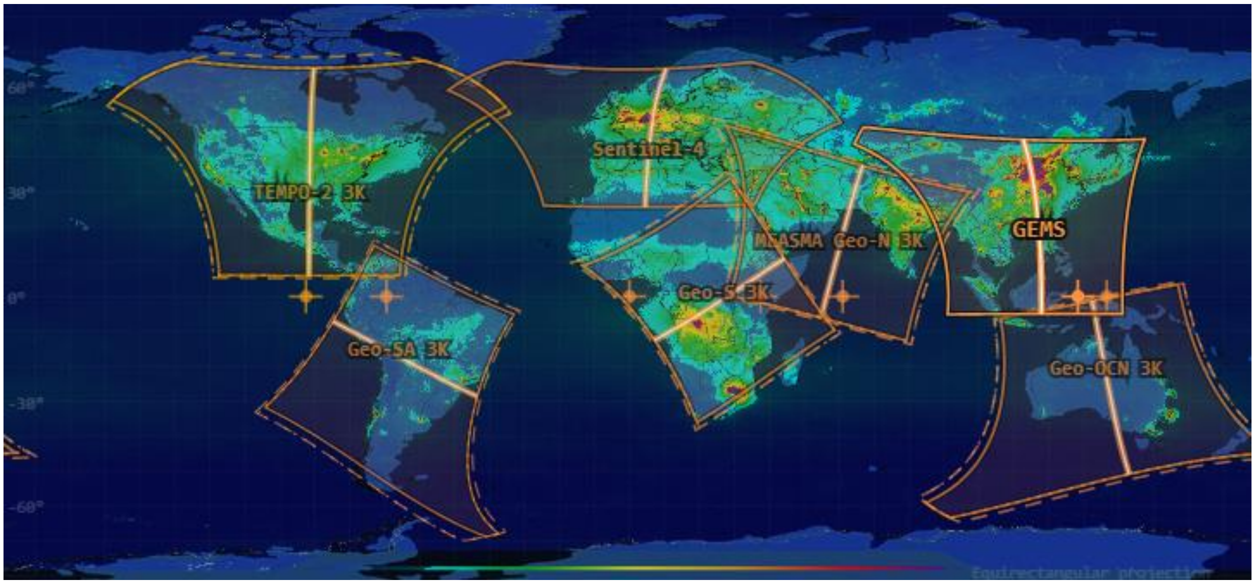

Figure 2. Vision for an expanded global geostationary air quality constellation, the ‘Geo-Belt’ overlaid on a map of global tropospheric NO_2 concentrations. The original GeoAQ Constellation satellites and their follow-ons are expanded by four new platforms: Geo SA (South America), Geo S (Africa), MEASMA Geo N (Middle East and India), and Geo OCN (Oceania) to extend this critical capability and achieve continuous, hourly monitoring of short-lived pollutants across a majority of the Earth’s populated surface.

As illustrated, this strategic expansion, the ‘Geo-Belt’, aligns continuous satellite coverage with the severe, under-monitored pollution hotspots of in unmonitored regions extending the capability of daytime diurnal monitoring to the vast majority of the Earth's populated surface. A dedicated **Africa (Geo S)** satellite is urgently needed as the continent rapidly urbanizes and transitions from seasonal biomass burning to anthropogenic fossil fuel emissions. African $PM_{2.5}$ levels far exceed WHO guidelines (Abera et al., 2021), and satellite estimates reveal that $PM_{2.5}$ associated infant mortality in the region is double standard global estimates (Heft-Neal et al., 2018). Continuous observations are vital to design targeted health interventions.

For the **Middle East and India (MEASMA Geo N)**, continuous monitoring is essential to track soaring urban NO_2 and complex particulate matter mixtures. In the Middle East, sustained $PM_{2.5}$ exposure is a staggering public health crisis, contributing to approximately 389,000 deaths in 2019 alone (Faridi et al., 2023). Similarly, India experiences some of the highest global $PM_{2.5}$ exposures, driving severe respiratory diseases and premature mortality (Chatterjee et al., 2023; Vohra et al., 2021, 2022).

A **South America (Geo SA)** platform will allow scientists to disentangle overlapping urban plumes, soil NO_x, and massive Amazonian wildfire emissions (Fioletov et al., 2022; Chen et al., 2023). High-cadence data is required to evaluate exposure-relevant ozone levels and support actionable, accountable public health policies (Huber et al., 2026).

Finally, an **Oceania (Geo OCN)** satellite is vital for tracking rapidly expanding, pyro-convective megafires that trigger profound public health crises, such as the thousands of cardiovascular and respiratory hospitalizations caused by the 2019–2020 bushfires (Borchers Arriagada et al., 2020). It will also resolve the region's unique photochemistry, where biogenic VOCs drive severe, localized ozone episodes (Utembe et al., 2018).

Together, this expanded constellation will provide the hourly, actionable exposure data required to protect vulnerable populations worldwide.

7. A Tale of Two Hemispheres: The Impact of Geographic Measurement Gaps

Relying exclusively on Low Earth Orbit (LEO) observations leaves blind spots across the Southern Hemisphere, demonstrating that periodic satellite snapshots cannot adequately substitute for continuous diurnal monitoring. This limitation is clearly illustrated in Figure 3 which maps the diurnal variation of aerosol optical depth in the Amazon. Because fire intensity, emission rates, and boundary layer dynamics fluctuate rapidly and intensely throughout the day, continuous observation is essential.

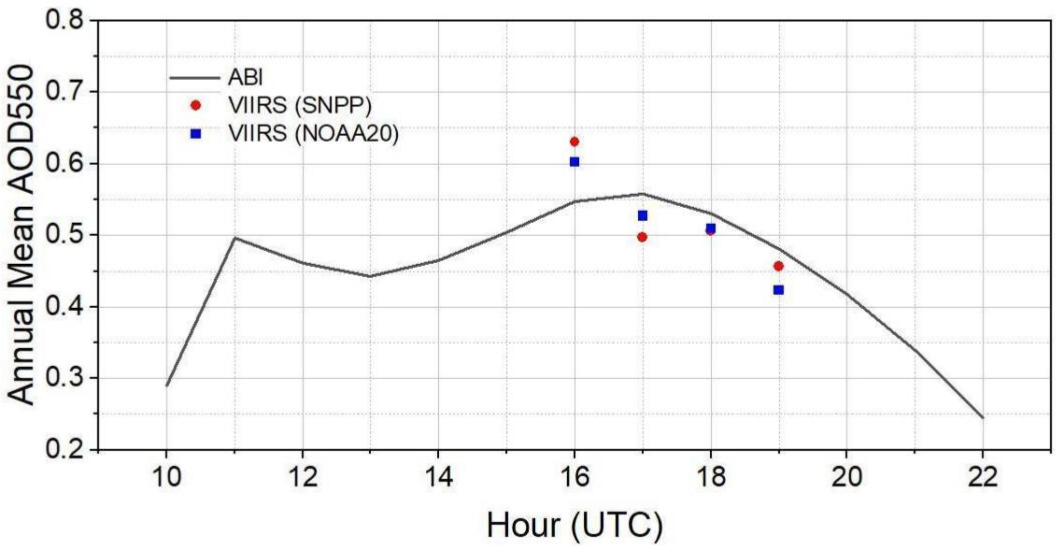

Figure 3. Diurnal variation of 2024 annual mean aerosol optical depth observed from ABI on NOAA's GOES-19 satellite shown in solid line with two VIIRS instruments on NOAA-20 and Suomi NPP observing aerosol optical depth over a specific time during the afternoon overpasses. VIIRS observations come from three overpasses for SNPP and four for NOAA-20. Note LEOs can provide multiple observations for the same region, especially at high latitudes, due to overlapping orbits but observations are made with different geometries. Observations reported here are for 70°W-60°W, 15°S-5°S (Ref).

Even with two separate VIIRS instruments actively monitoring the region, their staggered, infrequent overpasses fail to capture the full extent and rapid evolution of the smoke's daily cycle. By missing the peak emission hours and the subsequent transport of these hazardous plumes, this reliance on LEO architectures ultimately restricts our ability to accurately assess regional air quality, model short-term chemical transport, and issue timely public health warnings.

These dense diurnal observations identify previously unrecognized polluted hotspots that lack ground-level sensors (Siu et al., 2025). TEMPO also extends capabilities to trace gases like formaldehyde (HCHO), though continuous ground-based validation remains essential to correct systematic biases (Ortega et al., 2026), and provides high-cadence SO_2 measurements vital for tracking anthropogenic and volcanic plumes (Li et al., 2025). Maximizing these instruments, however, requires robust methodologies. Studies examining clear-sky versus cloudy-sky NO_2 differences using TROPOMI, TEMPO, surface monitors, and WRF-Chem models (Goldberg et al., 2025) highlight the necessity of proper calibration and accounting for environmental variables to refine top-down emissions inventories. Given the southward shift of global emissions and rapid population growth, coupled with sparse ground-based measurements, enhanced air quality monitoring is an urgent health imperative.

8. Geographic Gaps: Specific focus on Ozone (O3), Nitrogen dioxide (NO2) and Particulate Matter (PM) in Africa, Middle East, South America, India, Oceania

Ozone (O_3), nitrogen dioxide (NO_2), and fine particulate matter ($PM_{2.5}$) are primary criteria pollutants with profound human health impacts, originating from both vegetation fires and anthropogenic fossil fuel combustion. Globally, these emissions exhibit a stark hemispheric asymmetry as shown in Figure 4.

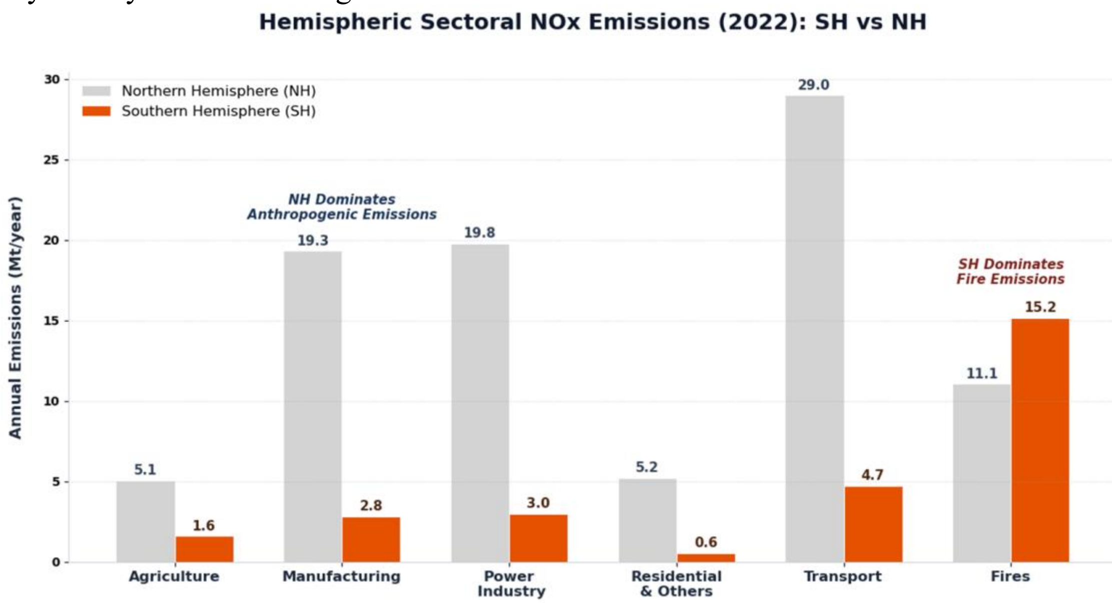

Figure 4. NOx emissions from different source sectors (Agriculture, Manufacturing, Power Industry, Transportation (gray bars) are higher than fire emissions in the northern hemisphere whereas in the southern hemisphere fire emissions are substantially higher than in the northern hemisphere. Anthropogenic emissions were obtained from the EDGAR database.

Northern Hemisphere pollution is primarily driven by fossil fuel consumption due to higher population densities, whereas Southern Hemisphere pollution is dominated by biomass burning. Because NO_2 is a short-lived precursor that drives the sunlight-dependent formation of both O_3 and ammonium nitrate aerosols (key components of $PM_{2.5}$), these pollutants are inextricably linked. These chemical interconversions occur rapidly, often over just a few hours. Consequently, single daily satellite snapshots are completely inadequate for capturing their dynamic diurnal cycles. Continuous, high-temporal-resolution observations from geostationary platforms are therefore essential to accurately track the fast-paced evolution of these interdependent pollutants and assess their true health impacts.

Surface concentrations of O_3, NO_2, and $PM_{2.5}$ exhibit significant spatial and diurnal variability driven by local emission sources, land use, and atmospheric processes (Huber et al., 2026). For instance, diurnal cycles are heavily dictated by the timing of agricultural fires or afternoon peaks in biogenic isoprene emissions. While regulatory actions and technological improvements have successfully reduced these pollutants in many countries, rapidly developing regions continue to face dangerously increasing exposure levels (HealthEffectsInstitute, 2025; Malashock et al., 2022; Vohra et al., 2022; WHO, 2023).

Furthermore, meteorological conditions, such as temperature, wind, humidity, and atmospheric stagnation play a critical role in influencing pollutant dispersion, deposition, and chemical transformation (Seinfeld & Pandis, 2016). This complex dynamic is increasingly compounded by both natural climate variability and anthropogenic climate change. These shifting climate factors alter the frequency and severity of heatwaves, droughts, and wildfire-favorable conditions, ultimately intensifying severe air pollution episodes across the globe (Byrne et al., 2024; Cooper et al., 2024; Lin et al., 2025; WHO, 2026).

In Africa, air quality challenges are dominated by high PM levels, largely from desert dust (e.g., Sahara), biomass burning (e.g., Savannah fires), and urban emissions. Limited monitoring infrastructure makes assessment difficult. NO_2 is rising in rapidly growing cities due to traffic and diesel use (Vohra et al., 2022), and industrial hotspots such as the highveld region in South Africa (Figure 5). O_3 formation is influenced by strong sunlight and precursor emissions from fires and urban pollution, often with weak regulatory control. Due to the predominant influence of fires, O_3 peaks in the dry burning season.
The Middle East experiences extreme PM concentrations driven by frequent dust storms and arid conditions. Urban NO_2 pollution is significant due to traffic, fossil-fuel-based energy systems, and extraction and refinement of crude oil. O_3 concentrations are often high because of intense solar radiation combined with anthropogenic precursor emissions, making photochemical smog a persistent issue. Air quality in South America varies widely: NO_2 and $PM_{2.5}$ in urban areas is elevated due to transport and industry, while rural regions are heavily impacted by seasonal biomass burning occurring in August-October (e.g., Amazon). O_3 pollution is a concern in large cities due to photochemical reactions and large influence from natural O_3 precursors like isoprene from the Amazon forest. Monitoring networks exist but remain spatially uneven, limiting the regional consistency and continuity of air-quality observations. India experiences some of the world's highest $PM_{2.5}$ exposure levels, arising from multiple sources, including residential fuel combustion, industry, power generation, transport and agricultural-residue burning (Chatterjee et al., 2023; Vohra et al., 2021). Rapidly growing cities in South Asia have also experienced increasing pollutant exposure and associated premature mortality (Vohra et al., 2022).

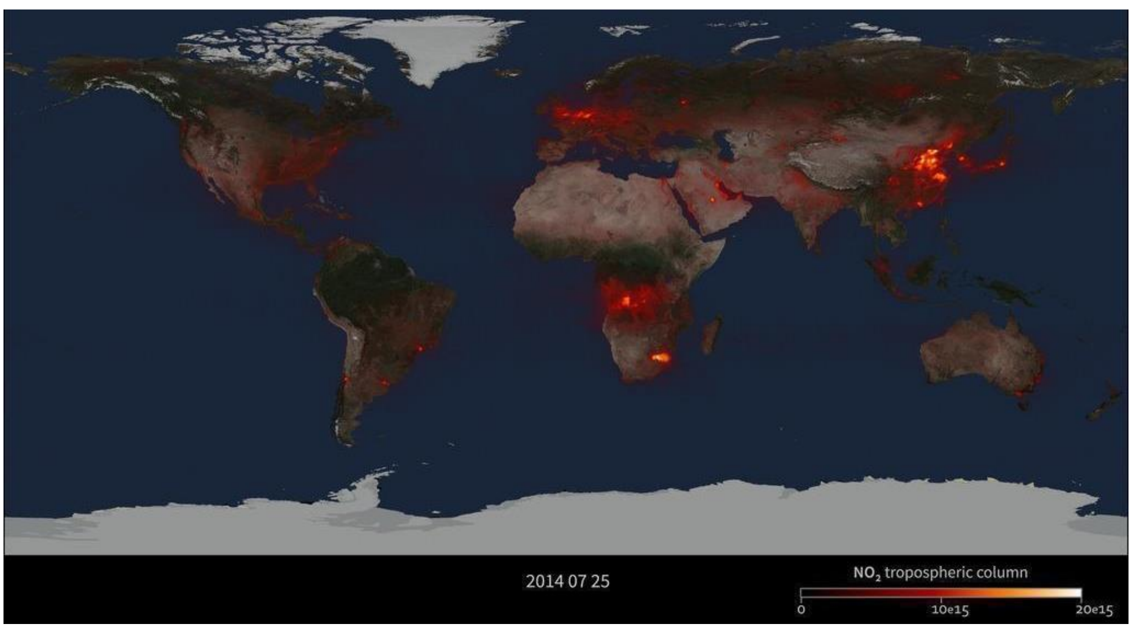

Figure 5. Tropospheric NO_2 column densities retrieved by the Ozone Monitoring Instrument (OMI) on July 25, 2014. High column densities over the South African Highveld region are associated with high power plant and industrial emissions in the region. Elevated column densities over south equatorial Africa are associated with dry season biomass burning activity

NO_2 concentrations are high in urban corridors due to dense traffic and energy production. O_3 is an emerging issue, especially in peri-urban and rural areas, where precursor transport and strong sunlight enhance formation. The Oceania region is characterized by generally lower pollution levels, but episodic events dominate. PM spikes occur during bushfires and dust events. NO_2 is mainly an urban traffic issue (e.g., Sydney, Melbourne). O_3 episodes can occur in cities under favorable meteorological conditions, though overall levels are lower compared to other regions. Unique to Oceania is the larger relative influence than other regions of oceanic emissions on regional O_3 and PM from natural sources, but also from anthropogenic activities at ports. NO_2, O_3 and PM are inextricably linked pollutants that must be observed concurrently to fully understand air quality. As a short-lived, highly reactive precursor, NO_2 drives the sunlight-dependent formation of both O_3 and ammonium nitrate aerosols which eventually manifest as $PM_{2.5}$. Because these chemical interconversions occur rapidly over a matter of hours, single daily satellite snapshots cannot capture their dynamic diurnal cycles. Continuous, high-temporal resolution observations from a geostationary platform or multiple satellites from LEO platforms are therefore essential to track the rapid evolution of these interdependent pollutants throughout the day, enabling a precise assessment of shifting geographic emissions and their health impacts.

9. Africa (Geo–S)

Traditionally, Africa's ozone (O_3) and particulate matter (PM) profiles have been dominated by desert dust and dry-season biomass burning, which release massive quantities of organic aerosols, VOCs, CO, and NO_x (Sauvage et al., 2005). Seasonal open fires remain the continent's largest source of NO_2 (Jaeglé et al., 2005). However, a 21st-century decrease in burned savanna area (Andela & Guido, 2014; Andela et al., 2017; Chen et al., 2023; Zubkova et al., 2019) has led to declining dry-season NO_2 concentrations over north equatorial savannas (Hickman et al., 2021; Ossohou et al., 2019) and a corresponding drop in surface O_3 (Donnou et al., 2024). Natural emissions also exert a profound influence. Soil microbes release massive NO pulses upon wet-season re-wetting, accounting for up to half of regional annual emissions (Hudman et al., 2012; Jaeglé et al., 2004; Vinken et al., 2014) and driving regional O_3 enhancements (Bouarar et al., 2011; Saunois et al., 2009). Furthermore, tropical Africa is a global hotspot for aloft NO_x generated by lightning (Albrecht et al., 2016; Cecil et al., 2014), which is highly efficient at O_3 production and is increasing in frequency due to climate change (Harel & Price, 2020; Qie et al., 2020). Cloud-sliced satellite data is currently used to constrain these lightning NO_x emissions in models (Marais et al., 2018). Ultimately, meteorology and non-NO_x sources continue to dominate the interannual variability of African O_3 (Qu et al., 2020).
Despite declining fire emissions (Figure 6), the air quality benefits are being rapidly erased by urbanization, population growth (Figure 7), and rising anthropogenic pollution (Liousse et al., 2014; Hickman et al., 2021). While African urban NO_2 levels remain less than half of those in Northern Hemisphere cities (Achakulwisut et al., 2019; Geddes et al., 2016) and historically lack the large combustion sources that titrate O_3 (Marais & Wiedinmyer, 2016), fossil fuel combustion is surging (Jaeglé et al., 2005; Schneider et al., 2015), particularly over the South African Highveld (Beirle et al., 2023; Lourens et al., 2012). From 2000 to 2019, urban NO_x increased 1–2% annually (Anenberg et al., 2022; Sicard et al., 2023), accelerating to 3–6% in the fastest-growing cities (Vohra et al., 2022). Consequently, large cities are shifting from NO_x-limited (Saunois et al., 2009; Marais et al., 2025) to NO_x-saturated O_3 production regimes (Vohra et al., 2022). The transition from fuelwood to charcoal (Bockarie et al., 2020), a projected doubling of electricity and transport NO_x by 2030 (Marais et al., 2019), and exponential soil NO spikes expected from increased fertilizer use (Hickman et al., 2017) point to rapidly deteriorating urban air quality.

This anthropogenic shift is severely compounding Africa's $PM_{2.5}$ public health crisis. Local urban PM sources, including aging vehicles, road dust, and charcoal production (Marais and Wiedinmyer, 2016; Bockarie et al., 2020; Keita et al., 2021, Bililign et al., 2024), mix with secondary PM formed from agricultural ammonia, NO_x, and VOCs (Hallquist et al., 2009; Shrivastava et al., 2017; Vakkari et al., 2018). Sulfates are largely localized to Rift Valley volcanoes, South African industry, and offshore powerships (Marais et al., 2022). Strikingly, only six sub-Saharan countries possess long-term PM data (Abera et al., 2021). Available data reveals city $PM_{2.5}$ ranges of 40–260 µg/m³, far exceeding WHO guidelines and US/European levels, with no exposre

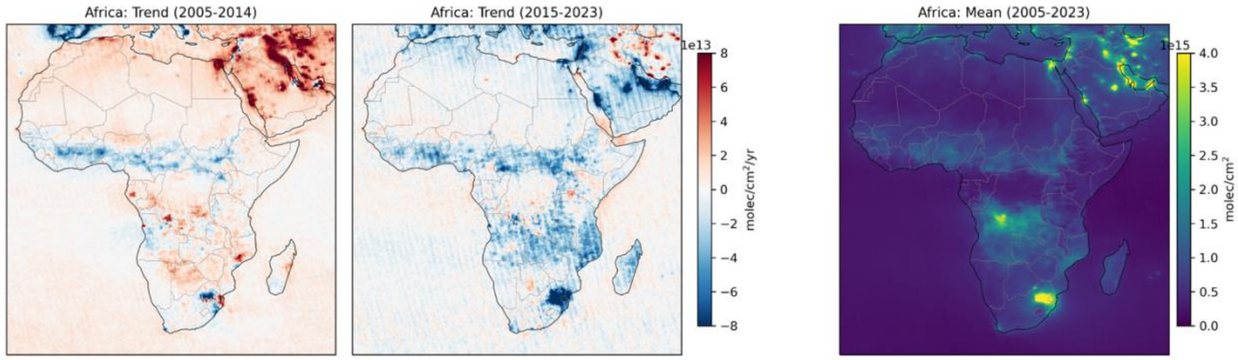

Figure 6. Trends and long-term mean in tropospheric NO_2 over Africa as observed by the Ozone Monitoring Instrument. [Note: these trends were calculated using L3 data. Because the OMI row anomaly affects different rows over the lifetime of the instrument, this analysis is based on a varying number of valid OMI observations over time, which may introduce artefacts into the analysis. As such, these should be treated as illustrative and interpreted with caution]

decline over the last 15 years (Abera et al., 2021). Because global models drastically underestimate this burden, satellite estimates reveal that a 10 µg/m³ $PM_{2.5}$ increase in Africa causes a 9% rise in infant mortality, double standard global estimates (Heft-Neal et al., 2018).

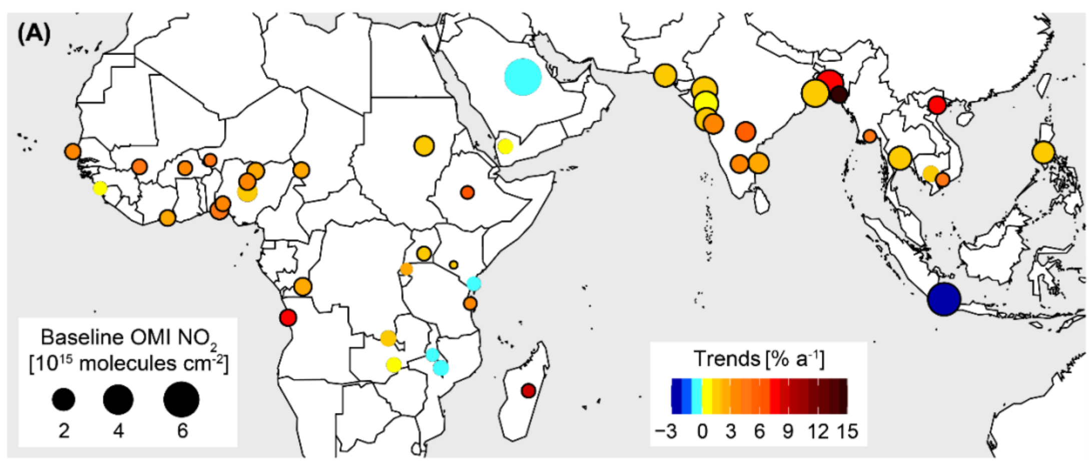

Figure 7. Changes in NO_2 concentrations across fast-growing tropical cities from 2005 to 2018. The diameter of each circle represents the baseline NO_2 level at the start of the observation period. The fill colors illustrate the direction and magnitude of the relative annual trends, with warm hues denoting an increase and cool hues signifying a decrease. Circles with borders indicate trends that are statistically significant at the 95% confidence interval.

While urban centers drive substantial global emissions (Crippa et al., 2021), Africa's specific contribution remains poorly quantified, largely because our understanding of its diurnal pollution variability is flawed. Recent studies in Addis Ababa (Figure 8) demonstrated that sharp morning

$PM_{2.5}$ peaks, driven by household cooking and rush-hour traffic, are missed entirely by standard models unless updated with hourly emission profiles (Li et al., 2024).

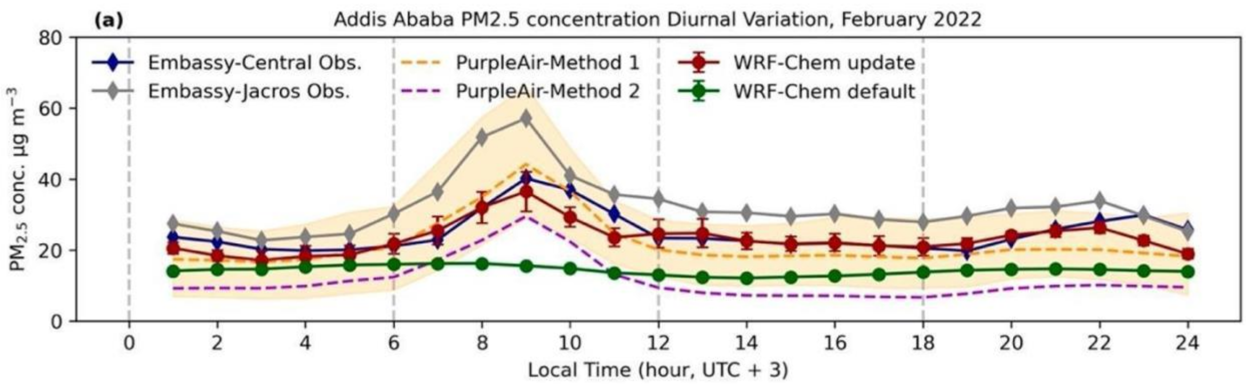

Figure 8. (a)Average diurnal variation of ground level PM2.5 concentration during February 2022 in Addis Ababa from surface measurements and UI-WRF-Chem simulations. Green dotted line represents the model simulation with default emission diurnal profile and red dotted line with updated diurnal profile. Blue and gray dotted lines represent the measurement from the Beta Attenuation Monitor (BAM) instrument at the U.S. Embassy Central and Jacrossite. Orange dashed line and Purple dashed line represent averaged diurnal variation from seven PurpleAir measurements using two different methods, and the orange shaded area is the range of PurpleAir diurnal variation from the first correction method. See details in (Li et al., 2024)

This highlights the critical need for continuous, diurnal satellite observations to accurately capture and mitigate Africa's escalating air quality crisis. Hourly adjustments can be achieved using an inversion method that applies hourly scaling factors (Li et al., 2024). Because Low Earth Orbit (LEO) satellites typically pass overhead near midday, they miss the critical early morning and late afternoon peaks in $PM_{2.5}$. Consequently, models that convert LEO aerosol optical depth (AOD) into surface $PM_{2.5}$ concentrations often significantly underestimate daily exposure, which can severely skew epidemiological studies of $PM_{2.5}$-related mortality. Utilizing continuous, diurnal AOD observations from geostationary platforms, complemented by surface measurements is essential to mitigate these uncertainties and capture the true public health burden.

10. Middle East and India (MEASMA Geo-N)

The Middle East and India are experiencing severe air quality degradation driven by surging anthropogenic emissions. In the Middle East, NO_X emissions stem almost entirely from fossil fuel combustion (Chen et al., 2023; Vinken et al., 2014), though lightning remains a major source along the Red Sea coast seasonally (Bond et al., 2002). Consequently, urban per capita NO_2 emissions in the Middle East are the highest globally (Fioletov et al., 2025). Between 2005 and 2014, regional NO_X emissions increased by 20% per decade (Miyazaki et al., 2017), driven by rapid expansion in urban centers, ports, power plants, and refineries (Barkley et al., 2017; Lelieveld et al., 2015; Sicard et al., 2023). While some cities saw increases exceeding 5% annually (Lelieveld et al., 2015; Schneider & van der A, 2012), regional trends show complex variability influenced by air quality controls, economic fluctuations, and armed conflict (Lelieveld et al., 2015; Miyazaki et al., 2017; Sicard et al., 2023). However, NO_2 over oil and power infrastructure continued rising steeply through at least 2015 (Barkley et al., 2017). This intense NO_2 loading, combined with atmospheric subsidence, generates a persistent year-round ozone hotspot exceeding 80 ppb (Lelieveld et al., 2009), leaving most countries failing the WHO 8-hour ozone guideline (WHO, 2026).

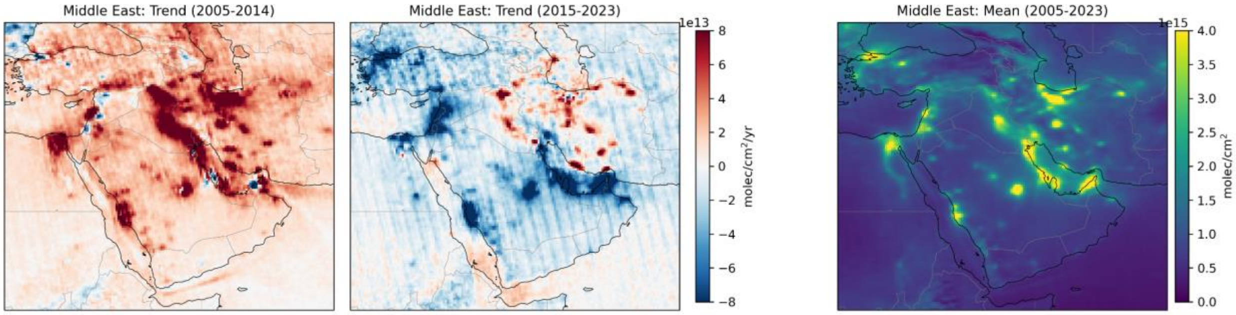

Figure 9. Trends and long-term mean in tropospheric NO2 over the Middle East as observed by the Ozone Monitoring Instrument (OMI).

Figure 9 shows the trends in the last two decades showing decreases in this decade and increases in the 2005-2015 decade using Level 3 OMI data. Because the OMI row anomaly affects different rows over the lifetime of the instrument, this analysis is based on a varying number of valid OMI observations over time, which may introduce artefacts into the analysis. As such, these should be treated as illustrative and interpreted with caution.

In contrast India has seen substantial tropospheric NO_2 increases over the past two decades (Ghude et al., 2013; Pathak & Kuttippurath, 2022; Singh et al., 2023; Vohra et al., 2022). Fast-growing Indian cities experience NO_2 increases up to 5% annually due to rising transportation and industrial combustion (Vohra et al., 2021). Satellite data reveals winter NO_2 peaks over the densely populated Indo-Gangetic Plain (Singh et al., 2023; Vohra et al., 2021), while pre-monsoon peaks in eastern and southern India are driven by coal-fired power plants and agricultural fires (Singh et al., 2023).

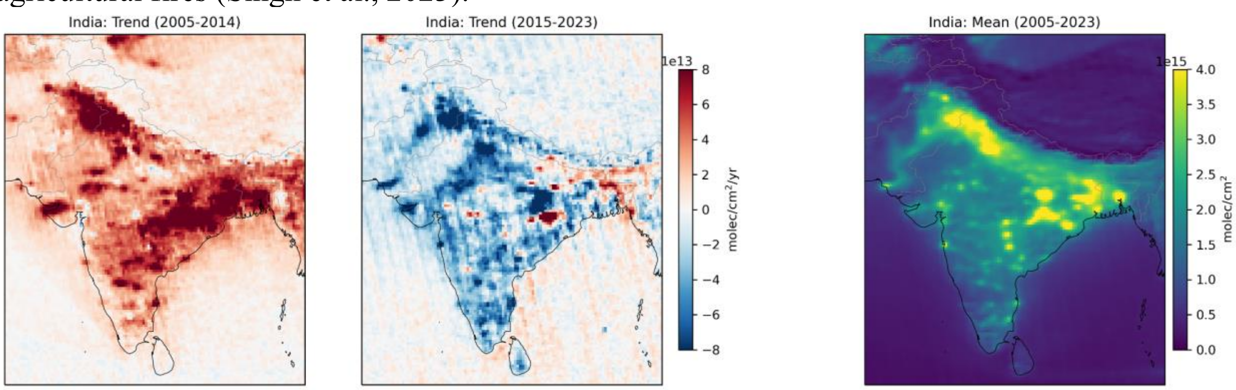

Figure 10. Trends and long-term mean in tropospheric NO2 over India as observed by the Ozone Monitoring Instrument. [Note: these trends were calculated using L3 data. Because the OMI row anomaly affects different rows over the lifetime of the instrument, this analysis is based on a varying number of valid OMI observations over time, which may introduce artefacts into the analysis. As such, these should be treated as illustrative and interpreted with caution].

Also note that in Figure 10, in many regions, the strong positive trends in tropospheric NO2 appear to have reversed starting in the mid-2010s. Because ground observations are heavily concentrated in urban areas (Vohra et al., 2025), satellite monitoring is crucial for tracking rural NO_2 growth, which is rising ~25% slower than in urban areas (Pathak & Kuttippurath, 2022). Ultimately, these Indian emissions drive significant O_3 enhancements, forming an "ozone river" extending over the Indian Ocean (Tocquer et al., 2015). Beyond $NO_2$and O_3, both regions face catastrophic particulate matter (PM) crises. In the Middle East and Eastern Mediterranean Region, anthropogenic pollution is layered over massive natural dust emissions. Windblown dust from the Tigris and Euphrates valleys and the Arabian Peninsula is mobilized by powerful shamal winds (Karagulian et al., 2019), accounting for roughly 51% of regional $PM_{2.5}$ exposure (Faridi et al., 2023). Individual transboundary dust storms push PM_{10} concentrations beyond 3,200 to 4,899 μg/m³ (Maleki et al., 2022), traverse countries (Hussein et al., 2020), and severely cut surface solar radiation (Karagulian et al., 2019). Layered upon this is the growing anthropogenic burden from urbanization, petrochemicals, vehicular traffic, and open waste burning (Shahid et al., 2024), making $PM_{2.5}$ a leading mortality risk that contributed to ~389,000 deaths in 2019 (Faridi et al., 2023; Shahid et al., 2024).

India experiences similarly elevated PM pollution that regularly exceeds WHO guidelines, altering the regional climate and radiation budget (Agarwal et al., 2024; Lin et al., 2022). Historical analyses show steady increases in $PM_{2.5}$ and O_3 from 1995 to 2014, driving regional mortality (Luo et al., 2025). Without policy interventions, $PM_{2.5}$ levels could elevate further by the 2050s (Pommier et al., 2018). India's PM sources are highly heterogeneous: industrial emissions are the primary domestic contributor (Venkataraman et al., 2018; Zhou et al., 2025), while household solid fuel combustion creates sharp daily pollution peaks tied to mealtimes (Rooney et al., 2019). Furthermore, groundwater conservation policies have delayed the rice growing season, pushing agricultural crop residue fires later into the year (Chang and Song, 2010). These delayed fires coincide with cooler temperatures and lower boundary layers, trapping smoke near the surface (Liu et al., 2022). This modifies aerosol optical properties and transports smoke across the Indo-Gangetic Plain (Kaskaoutis et al., 2014), extending southward to suppress the boundary layer in cities like Chennai (Ali et al., 2025). Secondary aerosol formation driven by photochemical reactions further interacts with the planetary boundary layer, causing atmospheric stagnation and prolonged haze (Agarwal et al., 2024; Lin et al., 2022).

To capture these highly dynamic crises, continuous observation is critical. While scientists utilize ground networks, low-cost sensors, chemical transport models, and remote sensing to bridge spatial gaps and optimize emission models (Kajino et al., 2025; Bali et al., 2019; Zhou et al., 2025), current polar-orbiting satellites provide only limited daily snapshots. They often underestimate emissions when obscured by clouds or smoke (Kajino et al., 2025) and cannot capture the rapid, 24- to 48-hour lifecycle of severe Middle Eastern dust storms (Karagulian et al., 2019; Maleki et al., 2022) or the daily mealtime emission spikes in India. Thus, continuous geostationary observations are vital to track these complex, hour-by-hour atmospheric hazards.

11. South America (Geo-SA)

South America's air quality is shaped by a highly complex, overlapping mix of massive biomass burning, intense natural biogenic emissions, and evolving urban anthropogenic sources. Deforestation and agricultural burning, particularly within the Amazon basin, are major sources of particulate matter (PM) and aerosols that profoundly alter regional climate, air quality, and the hydrological cycle (Artaxo et al., 2006). South and Central America account for roughly 8.6% of the global burned area (Chen et al., 2023) and produce about 15% of global wildfire emissions, driven largely by repeated deforestation fires (Morton et al., 2008; van der Werf et al., 2010), alongside significant agricultural and cerrado burning (Castellanos et al., 2014). Satellite observations reveal that NO_X emission factors from these fires are highly variable by season and fire type, meaning static inventories often misrepresent fire contributions during droughts (Castellanos et al., 2014). While the annual burned area decreased by roughly 2% yr^{-1} between 2001 and 2020 due to agricultural declines (Chen et al., 2023), anthropogenic climate change is estimated to have caused 28.9% more area to burn between 2003 and 2019 than would have occurred otherwise (Burton et al., 2024). Extreme events, such as the 2017 central Chile megafires, further compound this by producing massive regional plumes containing CO, aerosols, and O_3, severely perturbing radiation and boundary-layer dynamics (Lapere et al., 2021; Seguel et al., 2024).

In remote regions like the Amazon, the atmosphere's background oxidizing capacity is heavily driven by large soil NO_x emissions (Kaplan et al., 1988; Torres & Buchan, 1988; Verchot et al., 2000; Vinken et al., 2014; Liu et al., 2016; Shrivastava et al., 2019). Soil rewetting pulses account for about a third of annual NO_X emissions in dry forests (Davidson et al., 1991), though much of this is intercepted by the forest canopy (Jacob & Bakwin, 1991). Lightning serves as a minor NO_X source outside of the austral summer (Bond et al., 2002). Because of massive biogenic VOC emissions and modest NO_x levels, remote Amazonian regions are generally expected to be NO_X-limited (Tripathi et al., 2025). However, when urban NO_X plumes transport into these forested areas, they dramatically alter the local chemistry, driving secondary organic aerosol (SOA) and O_3 enhancements of 50–200% (Nascimento et al., 2022; Shrivastava et al., 2019; Wei et al., 2019). Overall, meteorology and non-NO_x sources tend to drive the interannual variability in O_3 more strongly than NO_X emissions alone (Qu et al., 2020). Figure 11 shows the NO2 trends in South America.

Urban pollution trends add another layer of complexity. Surface O_3 monitoring remains highly limited, but recent reviews indicate increasing exposure in subtropical/extratropical cities like Santiago and São Paulo, with little change in tropical, high-altitude cities like Bogotá and Quito (Seguel et al., 2024). While South American urban NO_2 levels are among the lowest globally (Fioletov et al., 2025), emissions can rival those of large North American and European cities (Beirle & Wagner, 2024; Rocha et al., 2022). Regionally, NO_X emissions were estimated to decrease by 12.2% per decade between 2005 and 2014 (Miyazaki et al., 2017). Yet, city-level trends vary: between 2000 and 2019, NO_2 increased by 1-2% yr^{-1} in over half of the continent's urban areas, with distinct increases in Bolivia, Peru, and Uruguay, but decreases in Venezuela (Sicard et al., 2023). Recent TROPOMI data (2019–2024) indicates aggregated urban NO_2 changes are not statistically significant continent-wide, though Santiago showed a notable decrease (Huber et al., 2026).

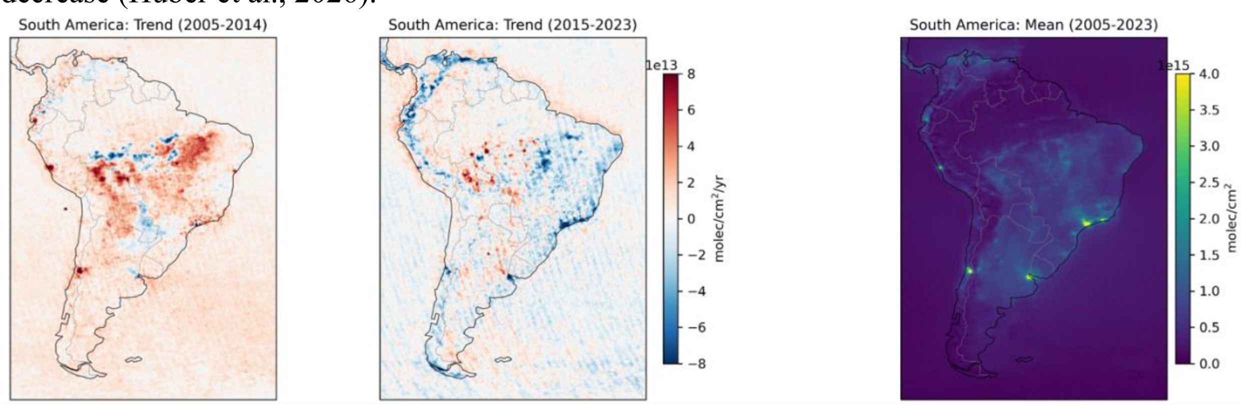

Figure 11. Trends and long-term mean in tropospheric NO2 over South America as observed by the Ozone Monitoring Instrument. [Note: these trends were calculated using L3 data. Because the OMI row anomaly affects different rows over the lifetime of the instrument, this analysis is based on a varying number of valid OMI observations over time, which may introduce artefacts into the analysis. As such, these should be treated as illustrative and interpreted with caution].

Because background, fire, lightning, and urban sources heavily overlap in South America, satellite NO_2 columns can be difficult to interpret. Fortunately, recent TROPOMI-based methods successfully decompose NO_2 into urban, industrial, and background components (Fioletov et al., 2022). This separation capability is crucial for accountability; during the COVID-19 lockdowns, urban NO_2 fell by 40–50% in step with mobility reductions while background levels remained

stable, demonstrating satellite nitrogen dioxide's effectiveness as an accountability tool for transportation and industrial policies (Fioletov et al., 2022; Huber et al., 2026).
Ultimately, managing this air quality requires navigating complex chemical regimes. Many better-monitored South American cities exhibit VOC-limited or NO_X-saturated behavior, meaning NO_x reductions alone can inadvertently increase O_3 under certain conditions (Cazorla et al., 2025; Seguel et al., 2024). Box models for Quito and Santiago confirm that while VOC reductions consistently lower O_3 production, NO_X reductions can actually spike morning O_3 in Santiago (Cazorla et al., 2025). This intricate chemical balance demands simultaneous, high-frequency observations of NO_2, VOC proxies like HCHO, O_3, aerosols, and meteorology data that a dedicated geostationary satellite would uniquely provide.

12. Oceania (Geo-OCN)

Oceania faces a highly complex atmospheric profile driven by immense biogenic emissions, shifting urban pollution, and catastrophic environmental events. Australia has the second-highest urban per capita NO_X emissions globally, yet soil and fire represent larger regional NO_X sources (Jaeglé et al., 2005), and continental background NO_X remains among the lowest in the world (Fioletov et al., 2025). Urban NO_X emissions in Australian cities grew by roughly 2% yr^{-1} from 2000–2010 before reversing to decrease by ~1% yr^{-1} from 2010–2019 (Miyazaki et al., 2017; Sicard et al., 2023), a downward trend that continues today (Fioletov et al., 2025). Over the same periods, New Zealand's urban emissions steadily decreased, while Papua New Guinea saw rapid urban NO_X growth that later slowed. Beyond urban centers, natural NO_X sources display distinct spatial and temporal patterns: lightning produces over 80% of NO_X during the northern Australian austral summer (Bond et al., 2002), while soil emissions, though modest compared to other global regions (Hudman et al., 2012), exhibit a pronounced seasonal cycle (Vinken et al., 2014) heavily linked to precipitation (Metz et al., 2023).
This NO_X landscape interacts with Oceania's uniquely massive biogenic volatile organic compound (BVOC) emissions to complicate regional ozone (O_3) dynamics. Australia's coastal cities border vast eucalyptus forests, which are among the globe's highest emitters of isoprene and monoterpenes (Utembe et al., 2018). Figure 12 shows the general trends in the NO2 means. Contradicting standard models, Australian monoterpene emissions are not solely light-dependent; they emit heavily during hot nights, fundamentally altering the expected diurnal cycle of precursor gases (Emmerson et al., 2016; Emmerson et al., 2018). During extreme heatwaves, these biogenic emissions spike exponentially (Utembe et al., 2018). Because regional airsheds are predominantly NO_X-limited, even modest anthropogenic NO_x from local traffic interacting with this massive natural VOC load triggers rapid, severe photochemical O_3 production (Paton-Walsh et al., 2019; Utembe et al., 2018). Figure 13 shows the trends in NO2 from the OMI instrument over the past two decades.

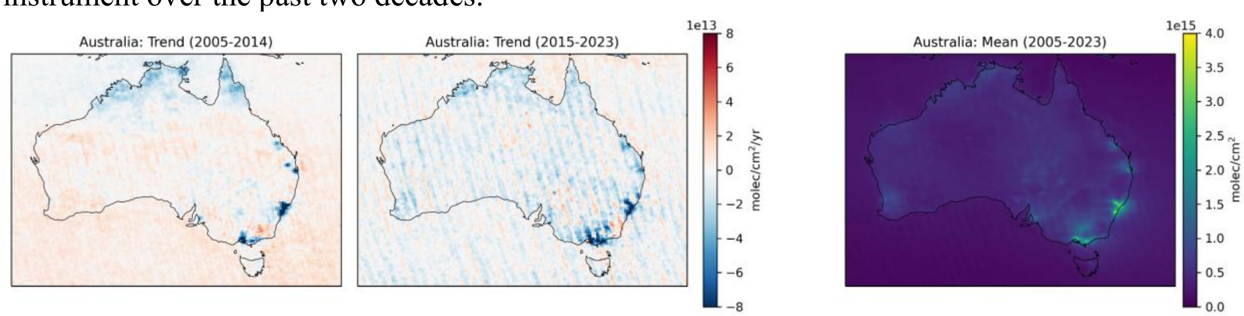

Figure 12. Trends and long-term mean in tropospheric NO2 over Australia as observed by the Ozone Monitoring Instrument. [Note: these trends were calculated using L3 data. Because the OMI row anomaly affects different rows over the lifetime of the instrument, this analysis is based on a varying

number of valid OMI observations over time, which may introduce artefacts into the analysis. As such, these should be treated as illustrative and interpreted with caution].

Urban photochemistry in the region is highly unusual. Instead of depleting at sunrise, nitrous acid (HONO) shows unexpected midday peaks, acting as a powerful, localized engine for hydroxyl radical (OH) production driven by uncharacterized photo-activated ground or soil emissions (Ryan et al., 2018). This chemistry is trapped and recirculated by complex coastal meteorology, including nocturnal katabatic drainage and afternoon sea breezes (Paton-Walsh et al., 2019). Compounding these modeling challenges is a shifting baseline: historically urban-centric monitoring limits the understanding of continental background O_3 (Riley et al., 2022), but recent rural data reveals background O_3 in eastern Australia is higher than regulatory models assumed and has steadily trended upward over two decades (Riley et al., 2022; Riley et al., 2023). Because standard ground-based UV monitors suffer from chemical interference during bushfires (Riley et al., 2022), high-resolution satellite instruments like TROPOMI are essential for mapping hotspots like formaldehyde (HCHO) to untangle this intricate biogenic chemistry (Ryan et al., 2020).

Compounding these photochemical challenges is Oceania's extreme particulate matter (PM) burden, dominated by mineral dust and biomass smoke (Yang et al., 2021). Synoptically driven dust storms routinely mobilize immense PM_{10} plumes from the western deserts and Lake Eyre Basin, devastating visibility and air quality in eastern coastal cities like Sydney (Attiya and Jones, 2022). Furthermore, while average burned area across Oceania decreased by ~3% yr^{-1} from 2001 to 2020 (Chen et al., 2023), the frequency of megafires and fall/winter fires has increased exponentially (Canadell et al., 2021). The catastrophic 2019–2020 "Black Summer" bushfires were unprecedented in both area (Rumpff et al., 2023; Wan et al., 2023) and high-severity occurrence (Collins et al., 2021). These megafires released immense NO_x emissions (Wan et al., 2023), driving Victorian NO_2 concentrations 12.7% higher than expected, though without substantial O_3 enhancements (Ryan et al., 2021), and unleashed toxic fine $PM_{2.5}$ that caused hundreds of excess deaths and thousands of hospitalizations (Borchers Arriagada et al., 2020). The pyro-convective scale of these plumes even crossed the Pacific to South America, depositing nutrients that triggered anomalous phytoplankton blooms in oligotrophic marine ecosystems (Li et al., 2021).

Additionally, stealthy, localized PM_{10} enhancements near open-cut coal mines pose a chronic health risk to rural communities; tracking this pollution requires advanced machine learning to separate mining dust from meteorological variables like soil moisture (Mallet, 2021). Ultimately, tracking the explosive, hour-by-hour transport of dust fronts and bushfire plumes, as well as resolving localized mining dust and complex coastal sea-breeze recirculation, is impossible with sparse ground networks and the once-daily snapshots of Low Earth Orbit (LEO) satellites (Attiya & Jones, 2022; Yang et al., 2021). A dedicated geostationary satellite is essential to continuously map aerosols, issue real-time public health warnings, and track transboundary ecological impacts (Li et al., 2021; Mallet, 2021).

13. Technical Feasibility and Implementation Considerations

Proposed GEO instruments to observe unmonitored regions of the world would draw on the heritage of GEMS, TEMPO and Sentinel-4, whose optical and orbital characteristics are shown in Table 1 These differ in their respective architectures due to science and mission requirements. GEMS and TEMPO are both step-stare instruments which use a scan mirror to point and dwell the imaging spectrometer's field of view while framing for an integration time that maximizes signal to noise ratio (SNR) while minimizing saturation. Frames are co-added on-board, and the raw data are downlinked to be processed into science products. The number of co-added frames contributes to the SNR optimization as it has an impact on read-out noise. The dwell time at each scan mirror position, scan time between positions, and return scan to the start position are the temporal constraints for defining the full field of regard in the East-West direction. Sentinel-4 also employs a scan mirror but uses a continuous push-broom scan pattern to cover the full field of regard from East to West. North-South coverage for all 3 instruments is constrained by the slit length, telescope focal length, and detector pixels.

While the scanning approaches are different, the three GeoAQ Constellation instruments all use custom frame-transfer charge-coupled devices (CCDs). Storage areas on the CCDs allow for frames to be read while continuing to integrate on the imaging regions. The spectral ranges of each instrument are constrained by the number of CCDs and the number of pixels per CCD as well as the spectral dispersion. GEMS has one CCD which covers the 300-500 nm range at 0.2 nm/pixel sampling (0.6 nm at full width half maximum (FWHM)). TEMPO has the same spectral dispersion but includes a second CCD to cover the 540-740 nm range for enhanced sensitivity to O3 nearer the surface. Sentinel-4 also has two CCDs, but covers 305-500 nm at 0.5 nm FWHM and 750-775 nm at 0.12 nm FWHM. As mentioned above, Sentinel-4 prioritizes the NIR at very high spectral resolution and their spectral range is made possible with two spectrometers. TEMPO only uses one spectrometer but has a specialized grating to accommodate such a large range and forgoes the near infra-red (NIR) part of the spectrum.

Table 1: Key Parameters of GeoAQ Constellation Instruments

Parameter	GEMS	TEMPO	Sentinel-4
Wavelength Range	300-500 nm	290-490, 540-740 nm	305-500, 750-775 nm
Spectral Resolution	0.6 nm (0.2 nm / pixel)	0.6 nm (0.2 nm / pixel)	0.5 nm (0.125m/pixel), 0.12 nm (0.04 nm/pixel)
N/S Field of View (Swath)	7.79°	4.76°	4.0°
E/W Field of Regard	11.5°	14.4°	13.8°
Nominal Spatial Sampling Distance	7 km x 8 km at 38° N	2.1 km x 4.7 km at 33.5°N	8 km x 8 km at 45°N
Detector Imaging Dimensions (Spatial x Spectral)	1028 x 2048	1028 x 2048, 1028 x 2048	600 x 1290, 600 x 713

These instrument differences offer opportunities to evaluate and leverage different priorities for different regions. Geographical extent is likely the biggest driver for future architecture. Coverage larger than the current fields of regards with the current on-orbit technology would require conceding on spatial resolution and/or temporal revisit. One of the largest drivers for new GEO architectures is the larger-format Complementary Metal-Oxide-Silicon (CMOS) detectors. With upwards of 3000-4000 pixels, the possibility of larger fields of regards from a single instrument become more feasible. To measure over landmasses larger than the current FORs in the current GeoAQ Constellation, one could consider longer revisits to accommodate larger scan ranges. These priorities should be considered for specifying mission requirements. Figure 13 shows an ideal orbital configuration for the satellite constellation of the Geo-Belt.

Figure 13. Vision for an expanded global geostationary air quality constellation, the 'Geo-Belt' overlaid on a map of global tropospheric NO_2 concentrations. The original GeoAQ Constellation satellites and their follow-ons are expanded by four new platforms: Geo SA (South America), Geo S (Africa), MEASMA Geo N (Middle East and India), and Geo OCN (Oceania) to extend this critical capability and achieve continuous, hourly monitoring of short-lived pollutants across a majority of the Earth's populated surface. 3K denotes the 3000 pixels afforded by the new CMOS detectors.

14. Addressing High-Latitude Observing Gaps with Inclined Geosynchronous Orbits (IGOs)

While geostationary (GEO) orbits provide the advantage of frequent temporal revisit rates, their equatorial alignment degrades data quality poleward of ~58° latitude due to extreme view zenith angles. Consequently, critical high-latitude regions sit at the absolute limit of current observing ranges, such as TEMPO's view of the Canadian oil sands (57°N). Continuous monitoring of these high latitudes is increasingly vital, as intensifying boreal megafires and oil sands excavation drive severe air pollution. This localized pollution drastically degrades regional air quality and disproportionately threatens vulnerable, remote populations who lack robust ground-based monitoring infrastructures.

To observe these circumpolar regions, highly elliptical orbits (HEO) are often proposed, as two HEO satellites can provide quasi-geostationary coverage. Space agencies globally have considered HEO missions (Trichtchenko et al., 2014), and the World Meteorological Organization (WMO) recommends HEO for continuous high-latitude viewing in its Vision for the Integrated Observing System (WIGOS) in 2040 (WMO 2019). Canada has specifically explored HEO for atmospheric composition monitoring (Nassar et al., 2019; Nassar et al., 2023). However, Canada's current Arctic Observing Mission (AOM) concept prioritizes meteorology and infrared sounding over UV-visible spectrometers. While AOM will successfully measure aerosol optical depth (AOD) and gases like CH_4 and NH_3, it will miss critical pollutants like NO_2 and HCHO.

.

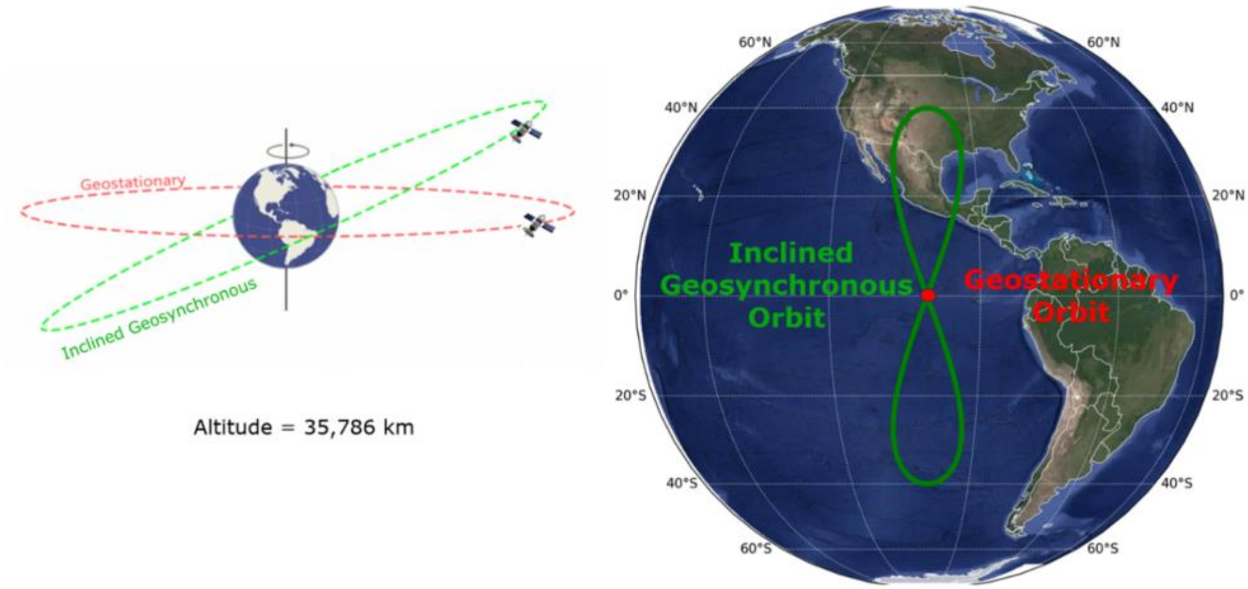

Figure 14 An inclined geosynchronous orbit (IGSO) is compared with a common GEO (left) and their ground tracks (right). Both orbits have the same altitude (35,786 km) and a period synchronized with Earth's rotation, but the IGSO has an orbit track that traces out at an analemma with highest latitude equal to the orbital inclination.

To provide observations in very high latitudes not covered by the measurements of the GeoAQ Constellation (*cf.* Figure 1), Inclined Geosynchronous Orbits (IGOs) offer a solution. Operating at GEO altitude (35,786 km) but with a non-zero inclination, an IGO traces a figure-8 analemma daily. IGOs are ideal for daytime observations focused on a single hemisphere. For instance, an IGO satellite with a 30–40° inclination could cover the U.S., Canada, and Mexico with vastly improved viewing angles compared to standard GEOs, achieving the same revisit rates far more efficiently than deploying multiple HEO satellites.

IGOs also present distinct operational advantages. By maintaining a constant altitude, they easily avoid the Van Allen radiation belts that constrain HEO eccentricities. Furthermore, the emergence of cost-effective micro-GEO buses makes stand-alone IGO air quality missions economically viable. Finally, as Low Earth Orbit (LEO) becomes increasingly congested with mega-constellations and orbital debris, exploiting higher, less crowded orbits like IGOs is a highly advisable strategy for the future of atmospheric monitoring.

15. Ground-Truthing the Geo-Belt: Expanding Surface Monitoring Infrastructure

The success of geostationary missions like GEMS, TEMPO, and Sentinel-4 relies heavily on reliable, co-located surface observations to "ground truth" satellite retrievals of pollutants like O_3, NO_2 and $PM_{2.5}$. Ironically, the regions that most urgently require satellite monitoring, such as Africa, South America, the Middle East, India, and to some extent Oceania, also suffer from severe ground-level data gaps, presenting a major challenge for validation. Addressing this requires a dedicated, preemptive program to leverage existing infrastructure, establish new observation 'super sites', and train local scientists to ensure the long-term sustainability of these networks.

A survey of current global networks provides a foundational starting point for data assimilation but also highlights critical regional blind spots. For example, distribution maps of the WMO Global Atmosphere Watch (GAW, Figure 15) stations, the Pandonia Global Network (PGN, Figure 16) for Pandora instruments, and the Tropospheric Ozone Assessment Report database starkly illustrate the lack of surface ozone and atmospheric composition monitoring across the Global South. Furthermore, while MAX-DOAS instruments provide valuable measurements of HCHO, NO_2, and total column O_3 (with some data accessible via the FRM4DOAS project), they currently lack the global coordination seen in networks like Pandonia. Figure 15 shows the publicly available operational WMO GAW stations making at least one measurement of atmospheric composition around the world, illustrating the relative scarcity of observations in the southern Hemisphere, South Asia and the Middle East.

Figure 15. Global distribution of operational WMO Global Atmosphere Watch (GAW) stations making at least one measurement of atmospheric composition. Source: GAWSiS, https://gawsis.meteoswiss.ch/GAWSIS

Conversely, the Surface Particulate Matter Network (SPARTAN) demonstrates how targeted ground networks can successfully enhance satellite capabilities. SPARTAN is a global network that evaluates and improves satellite-based $PM_{2.5}$ estimates by co-locating air samplers, which measure $PM_{2.5}$ mass and detailed chemical composition, with sun photometers that measure aerosol optical depth (AOD) at established AERONET sites. This specific combination provides the critical empirical data necessary to translate satellite AOD column measurements into accurate ground-level $PM_{2.5}$ concentrations (Snider et al., 2015). SPARTAN deploys these stations in highly populated, historically under-monitored regions.
The network archives standardized data on components like black carbon, trace metals, and inorganic ions, ultimately improving both global chemical transport models and public health exposure estimates (Weagle et al., 2018).

Figure 16. Current global distribution of Pandora instruments. Source: Pandonia Global Network (PGN), https://www.pandonia-global-network.org/home/

The AErosol RObotic NETwork (AERONET, Figure 17) is a globally distributed network of ground-based sun-and-sky radiometers operated by NASA, and numerous international partners to monitor atmospheric aerosols. Recognized as the gold standard for aerosol measurement, AERONET instruments continuously measure aerosol optical depth (AOD) and derive advanced optical, microphysical, and radiative properties across hundreds of sites worldwide. Because it provides highly accurate, continuously calibrated, and open-access data, AERONET serves as the primary "ground truth" for validating satellite aerosol retrievals and evaluating chemical transport models, making it an indispensable tool for understanding regional air pollution, aerosol transport, and climate forcing.

For the proposed expansion of the geostationary GeoAQ Constellation across the Global South, AERONET will be a critical tool for continuous validation. Because the new GEO satellites will provide hourly observations of aerosol optical depth (AOD) rather than once-daily snapshots, AERONET’s high-frequency daytime measurements are uniquely suited to validate the rapid diurnal variations captured from space such as morning pollution spikes, fast-moving dust storms, or evolving wildfire smoke plumes. By anchoring these continuous GEO retrievals with highly accurate AERONET ground data, scientists can significantly refine the algorithms used to translate satellite column AOD into ground-level $PM_{2.5}$ concentrations. Expanding AERONET and co-located PM sensor networks in under-monitored regions like Africa, South America, and the Middle East will ensure that the high-cadence data generated by the new GEO satellites is robust, accurate, and immediately useful for public health and policy decisions.

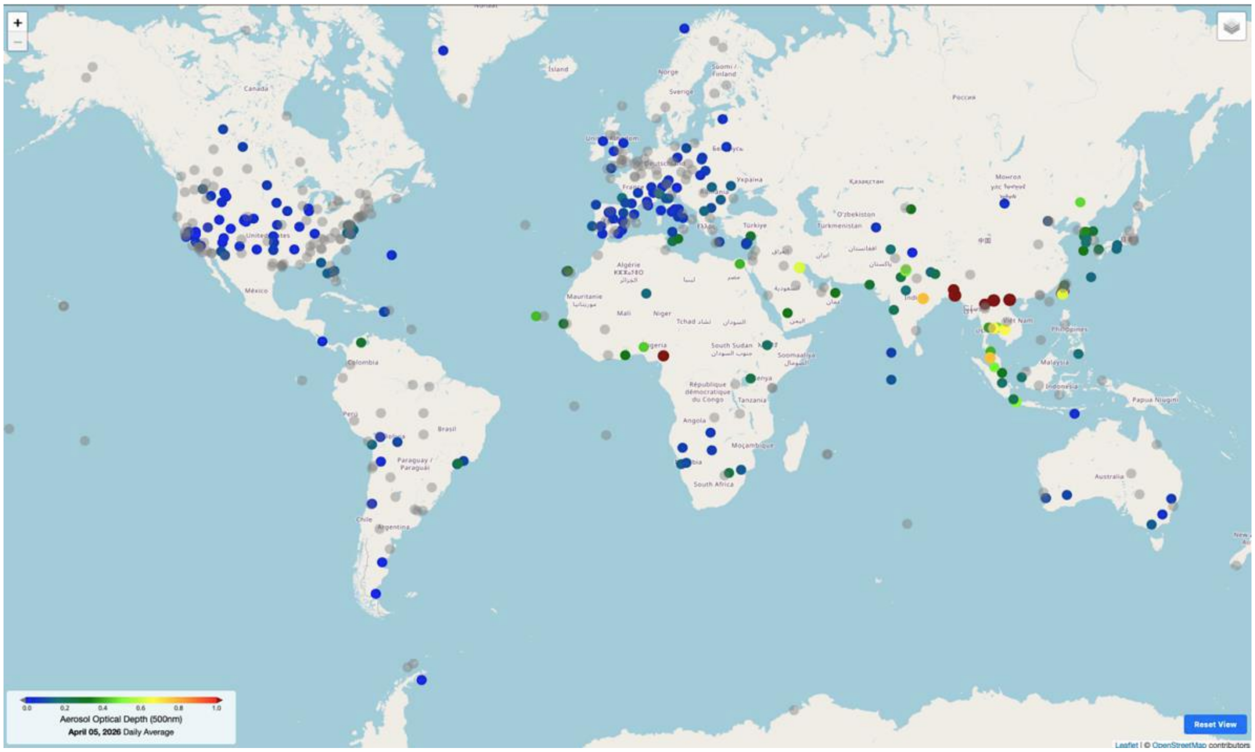

Figure 17. Distribution of AERONET sites on April 5, 2026 color coded by magnitude of the aerosol optical depth.

16. Advancing Predictive Capabilities: The Geo-Belt Satellites Integration in Atmospheric Modeling

Satellite-derived atmospheric composition products have fundamentally transformed the accuracy and reliability of chemical transport models (CTMs), numerical weather prediction (NWP), and air quality forecasting and reanalysis systems (e.g., Benedetti et al., 2018; Xian et al., 2019; Inness et al., 2019; Di Tomaso et al., 2022). Today, these observations play a central role across four major predictive frameworks:

First, in data assimilation systems, integrating variables like aerosol optical depth (AOD), aerosol layer height, NO_2 columns, and ozone profiles continuously corrects model states toward actual atmospheric conditions. This reduces uncertainties in pollutant concentrations and meteorological interactions, leading to measurable improvements in reproducing observed air pollution patterns (Inness et al., 2019; Di Tomaso et al., 2022). Second, these products enable robust emissions estimation. By providing 'top-down' estimates from space, satellites help quantify natural and anthropogenic emissions, identifying critical biases in traditional 'bottom-up' regional inventories. Third, advanced inverse modeling utilizes these datasets for source attribution, distinguishing between complex origins like biomass burning, dust transport, volcanic activity, and urban emissions to support targeted mitigation strategies (Wu et al., 2022). Finally, in forecast verification frameworks, models are routinely evaluated against satellite data to assess predictive skill, detect systematic biases, and refine representations of chemical reactions, aerosol dynamics, and boundary-layer processes (Akritidis et al., 2018; Eskes et al., 2024).

Looking ahead, the next generation of geostationary and high-resolution hyperspectral satellites is expected to significantly enhance these predictive capabilities. Improved spatial resolution and temporal cadence will allow models to capture street-level urban pollution gradients, rapidly changing emissions, and small-scale atmospheric processes like boundary-layer turbulence, deep convection, and haboobs. Furthermore, it will enable the resolution of episodic, high-impact phenomena such as wildfire-driven pyro convection. These observational leaps, operating in parallel with rapid advances in artificial intelligence, machine learning, and hybrid modeling (Bertrand et al., 2023; Gui et al., 2026), promise to further revolutionize the integration of satellite data into global and regional atmospheric prediction systems.

17. Strategic Implementation of the Geo-Belt: Policy, Partnerships, and Data Readiness

To realize the full societal benefit of the Geo-Belt, orbiting hardware must be paired with robust, on-the-ground implementation. This requires establishing equitable global partnerships, investing in comprehensive capacity building, and aligning with established international environmental frameworks. Ultimately, the success of this expanded constellation depends on transforming raw satellite observations into harmonized, decision-ready data that empowers policymakers, strengthens equitable air-quality governance, and protects public health worldwide.

a) Fostering Global Partnerships for Geo-Belt

Building the Geo-Belt into a sustainable, globally operating network requires a partnership framework grounded in equitable collaboration. By engaging regional stakeholders, including environmental and health agencies, meteorological services, research institutions, and civil society, across the entire process from problem definition to evaluation, the mission's objectives and data products can be tailored to actual regional decision-making contexts. This participatory model is vastly preferable to a purely top-down approach; sustained stakeholder involvement improves product relevance, usability, and long-term local ownership, ultimately lowering costs and building distributed expertise across regions rather than relying on a single set of institutions (Vargas et al., 2022).

To successfully foster this global cooperation, a multi-level consortium must be established. International space agencies (such as NASA, ESA, JAXA, and KASA) can provide essential mission expertise, calibration support, and interoperability standards, while regional and national institutions define priority pollutants and target policy applications. Concurrently, research institutes and private-sector actors will play crucial roles by providing data retrieval training, AI processing tools, and cloud-based infrastructure to empower local scientists and reduce operational burdens. Because the uptake of satellite data is often hindered by fragmented responsibilities, weak communication, and limited organizational capacity, overcoming these barriers requires formal, cross-sector working groups that unite data providers, regulators, health institutions, and academic analysts into strong, iterative expert networks (Potts et al., 2024).

Finally, this collaborative expansion should adopt a phased, staged pathway. Near-term efforts must prioritize regional pilot programs, validation campaigns, and interoperable data services. Fusing satellite observations with ground-based measurements and atmospheric models is widely used and essential for improving the spatial continuity, interpretability, and policy applicability of air-quality information while addressing the inherent limitations of any single data source (Diao et al., 2019). In the medium term, these collaborations can evolve into regional centers of excellence and shared data-processing hubs. Ultimately, this staged approach will build the long-term institutional and technical foundation necessary to support dedicated geostationary missions in the Southern Hemisphere and other under-observed regions, where sparse ground networks and a lack of geostationary coverage currently constrain scientific understanding and environmental monitoring (Paton-Walsh et al., 2022).

b) From Observation to Action: Policy Implications and Capacity Building

Air pollution remains a leading global health risk, yet many regions lack the ground-based monitoring systems necessary to manage it. GEO atmospheric composition observations are not merely scientific endeavors, but as essential public-interest infrastructure. By capturing diurnal emissions, tracking transboundary transport (such as wildfires and dust), and filling massive surface monitoring gaps, the Geo-Belt will yield compounding returns. It provides the critical exposure data required for epidemiology, empowers early warning systems, ensures equitable access to environmental monitoring, and removes the data-scarcity barriers that so often paralyze local policy action.

However, providing open access to satellite data is not enough to guarantee societal benefit. Robust capacity building is essential if Earth observation data is to successfully support science-based decision-making in practice (Kansakar & Hossain, 2016). Therefore, capacity building must be integrated as a core operational requirement of the Geo-Belt, rather than an afterthought. Successful frameworks already demonstrate this necessity: EUMETSAT's *Destination 2030* explicitly links the delivery of atmospheric services to a wider enabling environment, including digital infrastructure and dedicated capacity-building efforts with a particular focus on Africa (EUMETSAT, 2021). Similarly, the Copernicus CAMS National Collaboration Programme drives the national uptake of atmospheric products through co-designed activities, localized training, and seamless integration with existing in-situ monitoring networks (Copernicus, 2026). These established programs prove that atmospheric data becomes operationally valuable only when embedded within broader, user-facing services, such as public air quality indices, health-relevant tools, and policy-support platforms. Consequently, Geo-Belt requires investments that go beyond simply teaching users how to download data. A credible capacity-building package must cultivate the institutional, technical, and digital ecosystems necessary to transform raw satellite observations into trusted, actionable services. This includes sustained workforce development for analysts and regulators, supporting regional calibration and validation campaigns, creating open-access processing workflows, and establishing regional data hubs that can seamlessly convert atmospheric observations into policy-ready information.

c) Supporting Global Air Quality Frameworks and Collaborations

Air pollution is a systemic global challenge that arises from interconnected sources, including transport, industry, agriculture, and household combustion requiring highly coordinated international action. Organizations such as the United Nations Environment Programme (UNEP), the World Health Organization (WHO), the World Meteorological Organisation (WMO), and the Climate and Clean Air Coalition (CCAC) play central roles in strengthening air quality governance and mitigation strategies. Consequently, the Geo-Belt should not be framed as a standalone technical initiative, but rather as a foundational infrastructure designed to empower and strengthen these existing international efforts, particularly in under-monitored regions.

International conventions have historically driven crucial action on transboundary pollution. For example, the United Nations Economic Commission for Europe's (UNECE) Convention on Long Range Transboundary Air Pollution (LRTAP) and its European Monitoring and Evaluation Programme (EMEP) have successfully utilized monitoring and modeling to establish legally binding commitments for reducing emissions across borders. The GeoAQ Constellation is highly relevant to these frameworks, as it provides the robust, harmonized observational systems needed for transboundary assessment and comparable reporting. Even in regions lacking strong regulatory mechanisms like LRTAP, the Geo-Belt can provide the common evidence base necessary to foster emerging cross-border cooperation and shared monitoring standards. As such, the Geo-Belt is a global asset that is in the national interest of all countries.

Reliable data is the backbone of these global assessments. The WHO currently tracks global air quality through its database and analytical frameworks like the Data Integration Model for Air Quality (DIMAQ) (Shaddick et al., 2020), which fuses ground monitoring, satellite observations, and modeling to estimate population exposure. These efforts are complemented by the WMO's Global Atmosphere Watch (GAW) programme, which standardizes atmospheric composition measurements globally. With the global population projected to reach ~8.5 billion by 2030, massive populations in rapidly urbanizing regions remain at risk. To effectively address this, the Geo-Belt's must align directly with these established global systems, filling critical observational gaps rather than duplicating efforts. By integrating into the wider international data ecosystem, the GeoAQ Constellation will deliver interoperable, decision-relevant air-quality information to regions where sparse in situ networks currently constrain environmental governance.

d) The Need for Harmonized, Analysis-Ready Air Quality Data

The true policy value of Geo-Belt relies on its ability to translate raw satellite observations into trusted, decision-ready products. Raw measurements are rarely sufficient for policymakers; they require harmonized retrievals, explicit uncertainty quantification, and seamless integration into existing forecasting systems. Because satellite observations typically measure column-integrated data rather than direct surface concentrations, converting these measurements into usable air-quality indicators requires careful retrieval design and fusion with ground-based monitors and models. While data fusion improves spatial continuity and practical usability, its performance remains highly sensitive to data quality and the availability of validation data (Diao et al., 2019; Malings et al., 2020).

Therefore, harmonization must be a core design objective from the outset. Standardized retrieval methods ensure that products are comparable across different regions and over time. This is particularly critical in Africa and the Middle East, where high dust loading, bright surfaces, and sparse ground monitors create difficult retrieval conditions. Without harmonized and well-documented methods, the same pollutant fields can be interpreted differently, which undermines confidence and limits policy uptake (Paton-Walsh et al., 2022). Explicit uncertainty quantification must also be integrated so decision-makers understand confidence levels, especially since inconsistencies can arise even among publicly available products that use similar data sources (Diao et al., 2019).

Equally fundamental is robust validation. Satellite products only become trusted operational tools when supported by sustained calibration using ground-based reference sites. In under-observed regions like the Southern Hemisphere, a lack of validation infrastructure can become a severe bottleneck for the entire observing system's reliability (EUMETSAT, 2024). To maximize utility, interoperability must be a central operational principle. Products should be designed with common metadata standards to integrate effortlessly into national monitoring systems, much like the successful approach taken by CAMS (EUMETSAT, 2021).

The Geo-Belt offers an unprecedented opportunity to support the Sustainable Development Goals (SDGs), particularly in developing countries that often struggle with limited technical capacity and fragmented statistical systems (Andries et al., 2022). For example, Earth Observation and harmonized modeling can help localize SDG 11.6.2 (urban $PM_{2.5}$ and PM_{10} exposure), moving beyond simple national reporting to actively identifying pollution hotspots and guiding interventions (Bailey et al., 2023). Ultimately, GeoAQ Constellation products must go beyond being 'analysis-ready' for scientists to become 'decision-ready' for public authorities. Policymakers do not need raw data; they need timely, comparable formats like hotspot maps and transboundary diagnostics to support immediate action (Potts et al., 2024). The success of the

Geo-Belt will be judged by its ability to deliver authoritative, policy-relevant evidence that drives equitable air-quality governance worldwide.

18. Conclusion

The expansion of the geostationary air quality constellation into a comprehensive global "Geo-Belt" is an urgent scientific and public health imperative. Rapid urbanization, surging anthropogenic emissions, and intensifying climate-driven events across Africa, the Middle East, India, South America, and Oceania expose massive, vulnerable populations to hazardous levels of NO_2, O_3, and $PM_{2.5}$ (Abera et al., 2021; Faridi et al., 2023). Currently, the reliance on the once-daily snapshots of Low Earth Orbit (LEO) satellites and sparse surface monitoring networks fails to capture the rapid, diurnal evolution of these pollutants, leaving critical blind spots in global environmental governance and epidemiological impact assessments (Heft-Neal et al., 2018).

To address this, the global community must leverage the successful design and proven technological heritage of the foundational GeoAQ Constellation instruments: TEMPO, Sentinel-4, and GEMS (CEOS, 2019). Crucially, as we expand to new regions, we must also actively support the continuity of this existing Northern Hemisphere network. Because GEMS was the first of these observatories to launch, the prompt deployment of its successor, GEMS-2, is an urgent international priority to preserve the current constellation and maintain an unbroken climate data record (Yang et al., 2024). Building upon these pioneering spectrometer architectures to deploy similar geostationary platforms over the Global South will yield unprecedented insights into diurnal atmospheric chemistry. When integrated into advanced chemical transport models, these hourly observations will drastically reduce emission inventory biases, enhance predictive forecasting, and enable real-time, life-saving public health interventions (Inness et al., 2019; Di Tomaso et al., 2022; Shu et al., 2023).

However, realizing the full potential of the Geo-Belt requires more than orbiting hardware. It demands a holistic, collaborative approach that includes the expansion of ground-based validation networks, such as SPARTAN and AERONET, to accurately anchor satellite retrievals (Snider et al., 2015; Weagle et al., 2018). Furthermore, it necessitates the production of harmonized, uncertainty-aware data products to ensure interoperability and cross-regional comparability (Diao et al., 2019; Malings et al., 2020). Coupled with sustained institutional capacity building and integration into established global environmental frameworks (Shaddick et al., 2020), this expanded constellation will successfully transform raw satellite observations into decision-ready, actionable evidence (Potts et al., 2024). Ultimately, this coordinated global commitment is essential to drive equitable air-quality management and safeguard public health worldwide.

19. References

Abera, A., Friberg, J., Isaxon, C., Jerrett, M., Malmqvist, E., Sjöström, C., Taj, T., & Vargas, A. M. (2021). Air Quality in Africa: Public Health Implications. *Annual Review of Public Health*, *42*(Volume 42, 2021), 193-210. https://doi.org/https://doi.org/10.1146/annurev-publhealth-100119-113802

Achakulwisut, P., Brauer, M., Hystad, P., & Anenberg, S. C. (2019). Global, national, and urban burdens of paediatric asthma incidence attributable to ambient NO(2) pollution: estimates from global datasets. *Lancet Planet Health*, *3*(4), e166-e178. https://doi.org/10.1016/s2542-5196(19)30046-4

Albrecht, R. I., Goodman, S. J., Buechler, D. E., Blakeslee, R. J., & Christian, H. J. (2016). Where Are the Lightning Hotspots on Earth? *Bulletin of the American Meteorological Society*, *97*(11), 2051-2068. https://doi.org/https://doi.org/10.1175/BAMS-D-14-00193.1

Andela, & Guido. (2014). Recent trends in African fires driven by cropland expansion and El Niño to La Niña transition. *Nature Climate Change*, *4*(9), 791-795. https://doi.org/https://doi.org/10.1038/nclimate2313

Andela, Morton, D. C., Giglio, L., Chen, Y., van der Werf, G. R., Kasibhatla, P. S., DeFries, R. S., Collatz, G. J., Hantson, S., Kloster, S., Bachelet, D., Forrest, M., Lasslop, G., Li, F., Mangeon, S., Melton, J. R., Yue, C., & Randerson, J. T. (2017). A human-driven decline in global burned area. *Science*, *356*(6345), 1356-1362. https://doi.org/https://doi.org/10.1126/science.aal4108

Anderson, J. O., Thundiyil, J. G., & Stolbach, A. (2012). Clearing the Air: A Review of the Effects of Particulate Matter Air Pollution on Human Health. *Journal of Medical Toxicology*, *8*(2), 166-175. https://doi.org/10.1007/s13181-011-0203-1

Andries, A., Morse, S., Murphy, R. J., Lynch, J., & Woolliams, E. R. (2022). Using Data from Earth Observation to Support Sustainable Development Indicators: An Analysis of the Literature and Challenges for the Future. *Sustainability*, *14*(3), 1191. https://www.mdpi.com/2071-1050/14/3/1191

Anenberg, S. C., Mohegh, A., Goldberg, D. L., Kerr, G. H., Brauer, M., Burkart, K., Hystad, P., Larkin, A., Wozniak, S., & Lamsal, L. (2022). Long-term trends in urban NO2 concentrations and associated paediatric asthma incidence: estimates from global datasets. *The Lancet Planetary Health*, *6*(1), e49-e58. https://doi.org/https://doi.org/10.1016/S2542-5196(21)00255-2

Arosio, C., Sofieva, V., Orfanoz-Cheuquelaf, A., Rozanov, A., Heue, K. P., Loyola, D., Malina, E., Stauffer, R. M., Tarasick, D., Van Malderen, R., Ziemke, J. R., & Weber, M. (2025). Intercomparison of tropospheric ozone column datasets from combined nadir and limb satellite observations. *Atmos. Meas. Tech.*, *18*(14), 3247-3265. https://doi.org/10.5194/amt-18-3247-2025

Attiya, A. A., & Jones, B. G. (2022). An extensive dust storm impact on air quality on 22 November 2018 in Sydney, Australia, using satellite remote sensing and ground data. *Environmental Monitoring and Assessment*, *194*(6), 432. https://doi.org/10.1007/s10661-022-10080-1

Bailey, J., Ramacher, M. O. P., Speyer, O., Athanasopoulou, E., Karl, M., & Gerasopoulos, E. (2023). Localizing SDG 11.6.2 via Earth Observation, Modelling Applications, and Harmonised City Definitions: Policy Implications on Addressing Air Pollution. *Remote Sensing*, *15*(4), 1082. https://www.mdpi.com/2072-4292/15/4/1082

Barkley, M. P., González Abad, G., Kurosu, T. P., Spurr, R., Torbatian, S., & Lerot, C. (2017). OMI air-quality monitoring over the Middle East. *Atmos. Chem. Phys.*, *17*(7), 4687-4709. https://doi.org/https://doi.org/10.5194/acp-17-4687-2017

Bauer, S. E., Tsigaridis, K., & Miller, R. (2016). Significant atmospheric aerosol pollution caused by world food cultivation. *Geophysical Research Letters*, *43*(10), 5394-5400. https://doi.org/https://doi.org/10.1002/2016GL068354

Beirle, S., Borger, C., Jost, A., & Wagner, T. (2023). Improved catalog of NOx point source emissions (version 2). *Earth Syst. Sci. Data*, *15*(7), 3051-3073. https://doi.org/10.5194/essd-15-3051-2023

Beirle, S., & Wagner, T. (2024). A new method for estimating megacity NOx emissions and lifetimes from satellite observations. *Atmos. Meas. Tech.*, *17*(11), 3439-3453. https://doi.org/https://doi.org/10.5194/amt-17-3439-2024

Bililign, S., Brown, S. S., Westervelt, D. M., Kumar, R., Tang, W., Flocke, F., Vizuete, W., Ture, K., Pope, F. D., Demoz, B., Asa-Awuku, A., Levelt, P. F., Kalisa, E., Raheja, G., Ndyabakira, A., & Gatari, M. J. (2024). East African Megacity Air Quality: Rationale and Framework for a Measurement and Modeling Program. *Bulletin of the American Meteorological Society*, *105*(8), E1584–E1602. https://doi.org/10.1175/BAMS-D-23-0098.1

Bockarie, A. S., Marais, E. A., & MacKenzie, A. R. (2020). Air Pollution and Climate Forcing of the Charcoal Industry in Africa. *Environmental Science & Technology*, *54*(21), 13429-13438. https://doi.org/10.1021/acs.est.0c03754

Bond, D. W., Steiger, S., Zhang, R., Tie, X., & Orville, R. E. (2002). The importance of NOx production by lightning in the tropics. *Atmospheric Environment*, *36*(9), 1509-1519. https://doi.org/https://doi.org/10.1016/S1352-2310(01)00553-2

Borchers Arriagada, N., Palmer, A. J., Bowman, D. M., Morgan, G. G., Jalaludin, B. B., & Johnston, F. H. (2020). Unprecedented smoke-related health burden associated with the 2019–20 bushfires in eastern Australia. *Medical Journal of Australia*, *213*(6), 282-283. https://doi.org/https://doi.org/10.5694/mja2.50545

Bouarar, I., Law, K. S., Pham, M., Liousse, C., Schlager, H., Hamburger, T., Reeves, C. E., Cammas, J. P., Nédéléc, P., Szopa, S., Ravegnani, F., Viciani, S., D'Amato, F., Ulanovsky, A., & Richter, A. (2011). Emission sources contributing to tropospheric ozone over Equatorial Africa during the summer monsoon. *Atmos. Chem. Phys.*, *11*(24), 13395-13419. https://doi.org/https://doi.org/10.5194/acp-11-13395-2011

Bowdalo, D., Basart, S., Guevara, M., Jorba, O., Pérez García-Pando, C., Jaimes Palomera, M., Rivera Hernandez, O., Puchalski, M., Gay, D., Klausen, J., Moreno, S., Netcheva, S., & Tarasova, O. (2024). GHOST: a globally harmonised dataset of surface atmospheric composition measurements. *Earth Syst. Sci. Data*, *16*(10), 4417-4495. https://doi.org/10.5194/essd-16-4417-2024

Burnett, R., Chen, H., Szyszkowicz, M., Fann, N., Hubbell, B., Pope, C. A., Apte, J. S., Brauer, M., Cohen, A., Weichenthal, S., Coggins, J., Di, Q., Brunekreef, B., Frostad, J., Lim, S. S., Kan, H., Walker, K. D., Thurston, G. D., Hayes, R. B., Lim, C. C., Turner, M. C., Jerrett, M., Krewski, D., Gapstur, S. M., Diver, W. R., Ostro, B., Goldberg, D., Crouse, D. L., Martin, R. V., Peters, P., Pinault, L., Tjepkema, M., van Donkelaar, A., Villeneuve, P. J., Miller, A. B., Yin, P., Zhou, M., Wang, L., Janssen, N. A. H., Marra, M., Atkinson, R. W., Tsang, H., Quoc Thach, T., Cannon, J. B., Allen, R. T., Hart, J. E., Laden, F., Cesaroni, G., Forastiere, F., Weinmayr, G., Jaensch, A., Nagel, G., Concin, H., & Spadaro, J. V. (2018). Global estimates of mortality associated with long-term exposure to outdoor fine particulate matter. *Proceedings of the National Academy of Sciences*, *115*(38), 9592-9597. https://doi.org/doi:10.1073/pnas.1803222115

Burton, C., Lampe, S., Kelley, D. I., Thiery, W., Hantson, S., Christidis, N., Gudmundsson, L., Forrest, M., Burke, E., Chang, J., Huang, H., Ito, A., Kou-Giesbrecht, S., Lasslop, G., Li, W., Nieradzik, L., Li, F., Chen, Y., Randerson, J., Reyer, C. P. O., & Mengel, M. (2024). Global burned area increasingly explained by climate change. *Nature Climate Change*, *14*(11), 1186-1192. https://doi.org/https://doi.org/10.1038/s41558-024-02140-w

Byrne, B., Liu, J., Bowman, K. W., Pascolini-Campbell, M., Chatterjee, A., Pandey, S., Miyazaki, K., van der Werf, G. R., Wunch, D., Wennberg, P. O., Roehl, C. M., & Sinha, S. (2024). Carbon emissions from the 2023 Canadian wildfires. *Nature*, *633*(8031), 835-839. https://doi.org/10.1038/s41586-024-07878-z

Canadell, J. G., Meyer, C. P., Cook, G. D., Dowdy, A., Briggs, P. R., Knauer, J., Pepler, A., & Haverd, V. (2021). Multi-decadal increase of forest burned area in Australia is linked to

climate change. *Nature Communications*, *12*(1), 6921. https://doi.org/https://doi.org/10.1038/s41467-021-27225-4
Cao, H., Henze, D. K., Zhu, L., Shephard, M. W., Cady-Pereira, K., Dammers, E., Sitwell, M., Heath, N., Lonsdale, C., Bash, J. O., Miyazaki, K., Flechard, C., Fauvel, Y., Kruit, R. W., Feigenspan, S., Brümmer, C., Schrader, F., Twigg, M. M., Leeson, S., Tang, Y. S., Stephens, A. C. M., Braban, C., Vincent, K., Meier, M., Seitler, E., Geels, C., Ellermann, T., Sanocka, A., & Capps, S. L. (2022). 4D-Var Inversion of European NH3 Emissions Using CrIS NH3 Measurements and GEOS-Chem Adjoint With Bi-Directional and Uni-Directional Flux Schemes. *Journal of Geophysical Research: Atmospheres*, *127*(9), e2021JD035687. https://doi.org/https://doi.org/10.1029/2021JD035687
Castellanos, P., Boersma, K. F., & van der Werf, G. R. (2014). Satellite observations indicate substantial spatiotemporal variability in biomass burning NO_x emission factors for South America. *Atmos. Chem. Phys.*, *14*(8), 3929-3943. https://doi.org/https://doi.org/10.5194/acp-14-3929-2014
Cazorla, M., Trujillo, M., Seguel, R., & Gallardo, L. (2025). Comparative ozone production sensitivity to NOx and VOCs in Quito, Ecuador, and Santiago, Chile. *Atmos. Chem. Phys.*, *25*(13), 7087-7109. https://doi.org/10.5194/acp-25-7087-2025
Cecil, D. J., Buechler, D. E., & Blakeslee, R. J. (2014). Gridded lightning climatology from TRMM-LIS and OTD: Dataset description. *Atmospheric Research*, *135-136*, 404-414. https://doi.org/https://doi.org/10.1016/j.atmosres.2012.06.028
CEOS. (2011). *A Geostationary Satellite Constellation for Observing Global Air Quality: An International Path Forward*. Retrieved 02/05/2026 from https://ceos.org/document_management/Virtual_Constellations/ACC/Documents/AC-VC_Geostationary-Cx-for-Global-AQ-final_Apr2011.pdf
CEOS. (2019). *Geostationary Satellite Constellation for Observing Global Air Quality: Geophysical Validation Needs*. Retrieved 02/05/2026 from https://ceos.org/document_management/Virtual_Constellations/ACC/Documents/GEO%20AQ%20Constellation%20Geophysical%20Validation%20Needs%201.1%202Oct2019.pdf
Chang, K. L., Cooper, O. R., Gaudel, A., Petropavlovskikh, I., Effertz, P., Morris, G., & McDonald, B. C. (2024). Technical note: Challenges in detecting free tropospheric ozone trends in a sparsely sampled environment. *Atmos. Chem. Phys.*, *24*(10), 6197-6218. https://doi.org/https://doi.org/10.5194/acp-24-6197-2024
Chatterjee, D., McDuffie, E. E., Smith, S. J., Bindle, L., van Donkelaar, A., Hammer, M. S., Venkataraman, C., Brauer, M., & Martin, R. V. (2023). Source Contributions to Fine Particulate Matter and Attributable Mortality in India and the Surrounding Region. *Environmental Science & Technology*, *57*(28), 10263-10275. https://doi.org/10.1021/acs.est.2c07641
Chen, Y., Hall, J., van Wees, D., Andela, N., Hantson, S., Giglio, L., van der Werf, G. R., Morton, D. C., & Randerson, J. T. (2023). Multi-decadal trends and variability in burned area from the fifth version of the Global Fire Emissions Database (GFED5). *Earth Syst. Sci. Data*, *15*(11), 5227-5259. https://doi.org/https://doi.org/10.5194/essd-15-5227-2023
Cho, Y., Kim, J., Go, S., Kim, M., Lee, S., Kim, M., Chong, H., Lee, W. J., Lee, D. W., Torres, O., & Park, S. S. (2024). First atmospheric aerosol-monitoring results from the Geostationary Environment Monitoring Spectrometer (GEMS) over Asia. *Atmos. Meas. Tech.*, *17*(14), 4369-4390. https://doi.org/10.5194/amt-17-4369-2024
Choi, M., Kim, J., Lee, J., Kim, M., Park, Y.-J., Jeong, U., Kim, W., Holben, B., Eck, T., Lim, J., & Song, C.-K. (2015). GOCI Yonsei Aerosol Retrieval (YAER) algorithm and validation

during DRAGON-NE Asia 2012 campaign. *Atmospheric Measurement Techniques Discussions*, *8*. https://doi.org/10.5194/amtd-8-9565-2015
Clerbaux, C., Boynard, A., Clarisse, L., George, M., Hadji-Lazaro, J., Herbin, H., Hurtmans, D., Pommier, M., Razavi, A., Turquety, S., Wespes, C., & Coheur, P. F. (2009). Monitoring of atmospheric composition using the thermal infrared IASI/MetOp sounder. *Atmos. Chem. Phys.*, *9*(16), 6041-6054. https://doi.org/10.5194/acp-9-6041-2009
Collins, L., Bradstock, R. A., Clarke, H., Clarke, M. F., Nolan, R. H., & Penman, T. D. (2021). The 2019/2020 mega-fires exposed Australian ecosystems to an unprecedented extent of high-severity fire. *Environmental Research Letters*, *16*(4), 044029. https://doi.org/https://doi.org/10.1088/1748-9326/abeb9e
Cooper, O. R., Chang, K.-L., Bates, K., Brown, S. S., Chace, W. S., Coggon, M. M., Gorchov Negron, A. M., Middlebrook, A. M., Peischl, J., Piasecki, A., Schafer, N., Stockwell, C. E., Wang, S., Warneke, C., Zuraski, K., Miyazaki, K., Payne, V. H., Pennington, E. A., Worden, J. R., Bowman, K. W., & McDonald, B. C. (2024). Early Season 2023 Wildfires Generated Record-Breaking Surface Ozone Anomalies Across the U.S. Upper Midwest. *Geophysical Research Letters*, *51*(22), e2024GL111481. https://doi.org/https://doi.org/10.1029/2024GL111481
Copernicus. (2026). *CAMS National Collaboration Programme*. Retrieved 12/07/2026 from https://atmosphere.copernicus.eu/cams-national-collaboration-programme
Crippa, M., Guizzardi, D., Pisoni, E., Solazzo, E., Guion, A., Muntean, M., Florczyk, A., Schiavina, M., Melchiorri, M., & Hutfilter, A. F. (2021). Global anthropogenic emissions in urban areas: patterns, trends, and challenges. *Environmental Research Letters*, *16*(7), 074033. https://doi.org/https://doi.org/10.1088/1748-9326/ac00e2
Cuesta, J., Eremenko, M., Liu, X., Dufour, G., Cai, Z., Höpfner, M., von Clarmann, T., Sellitto, P., Foret, G., Gaubert, B., Beekmann, M., Orphal, J., Chance, K., Spurr, R., & Flaud, J. M. (2013). Satellite observation of lowermost tropospheric ozone by multispectral synergism of IASI thermal infrared and GOME-2 ultraviolet measurements over Europe. *Atmos. Chem. Phys.*, *13*(19), 9675-9693. https://doi.org/https://doi.org/10.5194/acp-13-9675-2013
Davidson, Phalen, R. F., & Solomon, P. A. (2005). Airborne Particulate Matter and Human Health: A Review. *Aerosol Science and Technology*, *39*(8), 737-749. https://doi.org/10.1080/02786820500191348
Davidson, E. A., Vitousek, P. M., Matson, P. A., Riley, R., García-Méndez, G., & Maass, J. M. (1991). Soil emissions of nitric oxide in a seasonally dry tropical forest of México. *Journal of Geophysical Research: Atmospheres*, *96*(D8), 15439-15445. https://doi.org/https://doi.org/10.1029/91JD01476
Diao, M., Holloway, T., Choi, S., O'Neill, S. M., Al-Hamdan, M. Z., Van Donkelaar, A., Martin, R. V., Jin, X., Fiore, A. M., Henze, D. K., Lacey, F., Kinney, P. L., Freedman, F., Larkin, N. K., Zou, Y., Kelly, J. T., & Vaidyanathan, A. (2019). Methods, availability, and applications of PM(2.5) exposure estimates derived from ground measurements, satellite, and atmospheric models. *J Air Waste Manag Assoc*, *69*(12), 1391-1414. https://doi.org/https://doi.org/10.1080/10962247.2019.1668498
Donnou, H. E. V., Akpo, A. B., Ossohou, M., Delon, C., Yoboué, V., Laouali, D., Ouafo-Leumbe, M., Van Zyl, P. G., Ndiaye, O., Gardrat, E., Dias-Alves, M., & Galy-Lacaux, C. (2024). Measurement report: Long-term measurements of surface ozone and trends in semi-natural sub-Saharan African ecosystems. *Atmos. Chem. Phys.*, *24*(23), 13151-13182. https://doi.org/https://doi.org/10.5194/acp-24-13151-2024

Emberson, L. (2020). Effects of ozone on agriculture, forests and grasslands. *Philosophical Transactions of the Royal Society A: Mathematical, Physical and Engineering Sciences*, *378*(2183). https://doi.org/10.1098/rsta.2019.0327
Emmerson, K. M., Cope, M. E., Galbally, I. E., Lee, S., & Nelson, P. F. (2018). Isoprene and monoterpene emissions in south-east Australia: comparison of a multi-layer canopy model with MEGAN and with atmospheric observations. *Atmos. Chem. Phys.*, *18*(10), 7539-7556. https://doi.org/10.5194/acp-18-7539-2018
Emmerson, K. M., Galbally, I. E., Guenther, A. B., Paton-Walsh, C., Guerette, E. A., Cope, M. E., Keywood, M. D., Lawson, S. J., Molloy, S. B., Dunne, E., Thatcher, M., Karl, T., & Maleknia, S. D. (2016). Current estimates of biogenic emissions from eucalypts uncertain for southeast Australia. *Atmos. Chem. Phys.*, *16*(11), 6997-7011. https://doi.org/10.5194/acp-16-6997-2016
EUMETSAT. (2021). *Destination 2030*. Retrieved 04/05/2026 from https://www-cdn.eumetsat.int/files/2021-09/EUMETSAT_Strategy_FULL_Online.pdf
EUMETSAT. (2024). *Report of the 16th EUMETSAT User Forum in Africa*. Retrieved 04/05/2026 from https://www-cdn.eumetsat.int/files/2025-01/Report%20of%20the%2016th%20EUMETSAT%20User%20Forum%20in%20Africa%20-%20EN%20-%20FINAL_1.pdf
Faridi, S., Krzyzanowski, M., Cohen, A. J., Malkawi, M., Moh'd Safi, H. A., Yousefian, F., Azimi, F., Naddafi, K., Momeniha, F., Niazi, S., Amini, H., Künzli, N., Shamsipour, M., Mokammel, A., Roostaei, V., & Hassanvand, M. S. (2023). Ambient Air Quality Standards and Policies in Eastern Mediterranean Countries: A Review [Review]. *International Journal of Public Health*, *Volume 68 - 2023*. https://doi.org/https://doi.org/10.3389/ijph.2023.1605352
Fioletov, McLinden, C. A., Griffin, D., Zhao, X., & Eskes, H. (2025). Global seasonal urban, industrial, and background NO2 estimated from TROPOMI satellite observations. *Atmos. Chem. Phys.*, *25*(1), 575-596. https://doi.org/https://doi.org/10.5194/acp-25-575-2025
Fioletov, V., Griffin, D., McLinden, C. A., Zhao, X., Nowlan, C., & Abad, G. G. (2025). Diurnal Variations in Background and Urban NO2 Estimated From TEMPO. *Geophysical Research Letters*, *52*(21), e2025GL117360. https://doi.org/https://doi.org/10.1029/2025GL117360
Fioletov, V., McLinden, C. A., Griffin, D., Krotkov, N., Liu, F., & Eskes, H. (2022). Quantifying urban, industrial, and background changes in NO2 during the COVID-19 lockdown period based on TROPOMI satellite observations. *Atmos. Chem. Phys.*, *22*(6), 4201-4236. https://doi.org/10.5194/acp-22-4201-2022
Fishman, J., Watson, C. E., Larsen, J. C., & Logan, J. A. (1990). Distribution of tropospheric ozone determined from satellite data. *Journal of Geophysical Research: Atmospheres*, *95*(D4), 3599-3617.
Fleming, Z. L., Doherty, R. M., von Schneidemesser, E., Malley, C. S., Cooper, O. R., Pinto, J. P., Colette, A., Xu, X., Simpson, D., Schultz, M. G., Lefohn, A. S., Hamad, S., Moolla, R., Solberg, S., & Feng, Z. (2018). Tropospheric Ozone Assessment Report: Present-day ozone distribution and trends relevant to human health. *Elementa: Science of the Anthropocene*, *6*. https://doi.org/https://doi.org/10.1525/elementa.273
Franco, B., Clarisse, L., Van Damme, M., Hadji-Lazaro, J., Clerbaux, C., & Coheur, P.-F. (2022). Ethylene industrial emitters seen from space. *Nature Communications*, *13*(1), 6452. https://doi.org/https://doi.org/10.1038/s41467-022-34098-8
Froidevaux, L., Kinnison, D. E., Gaubert, B., Schwartz, M. J., Livesey, N. J., Read, W. G., Bardeen, C. G., Ziemke, J. R., & Fuller, R. A. (2025). Tropical upper-tropospheric trends

in ozone and carbon monoxide (2005–2020): observational and model results. *Atmos. Chem. Phys.*, *25*(1), 597-624. https://doi.org/10.5194/acp-25-597-2025
Fu, D., Kulawik, S. S., Miyazaki, K., Bowman, K. W., Worden, J. R., Eldering, A., Livesey, N. J., Teixeira, J., Irion, F. W., Herman, R. L., Osterman, G. B., Liu, X., Levelt, P. F., Thompson, A. M., & Luo, M. (2018). Retrievals of tropospheric ozone profiles from the synergism of AIRS and OMI: methodology and validation. *Atmos. Meas. Tech.*, *11*(10), 5587-5605. https://doi.org/10.5194/amt-11-5587-2018
Gaudel, A., Cooper, O. R., Ancellet, G., Barret, B., Boynard, A., Burrows, J. P., Clerbaux, C., Coheur, P.-F., Cuesta, J., Cuevas, E., Doniki, S., Dufour, G., Ebojie, F., Foret, G., Garcia, O., Granados-Muñoz, M. J., Hannigan, J. W., Hase, F., Hassler, B., Huang, G., Hurtmans, D., Jaffe, D., Jones, N., Kalabokas, P., Kerridge, B., Kulawik, S., Latter, B., Leblanc, T., Le Flochmoën, E., Lin, W., Liu, J., Liu, X., Mahieu, E., McClure-Begley, A., Neu, J. L., Osman, M., Palm, M., Petetin, H., Petropavlovskikh, I., Querel, R., Rahpoe, N., Rozanov, A., Schultz, M. G., Schwab, J., Siddans, R., Smale, D., Steinbacher, M., Tanimoto, H., Tarasick, D. W., Thouret, V., Thompson, A. M., Trickl, T., Weatherhead, E., Wespes, C., Worden, H. M., Vigouroux, C., Xu, X., Zeng, G., & Ziemke, J. (2018). Tropospheric Ozone Assessment Report: Present-day distribution and trends of tropospheric ozone relevant to climate and global atmospheric chemistry model evaluation. *Elementa: Science of the Anthropocene*, *6*. https://doi.org/10.1525/elementa.291
Geddes, J. A., Martin, R. V., Boys, B. L., & van Donkelaar, A. (2016). Long-Term Trends Worldwide in Ambient NO2 Concentrations Inferred from Satellite Observations. *Environ Health Perspect*, *124*(3), 281-289. https://doi.org/https://doi.org/10.1289/ehp.1409567
Ghude, S. D., Kulkarni, S. H., Jena, C., Pfister, G. G., Beig, G., Fadnavis, S., & van der A, R. J. (2013). Application of satellite observations for identifying regions of dominant sources of nitrogen oxides over the Indian Subcontinent. *Journal of Geophysical Research: Atmospheres*, *118*(2), 1075-1089. https://doi.org/https://doi.org/10.1029/2012JD017811
Goldberg, D. L., Nawaz, M. O., Lyu, C., He, J., Carlton, A. G., Kondragunta, S., & Anenberg, S. C. (2025). Clear-sky and cloudy-sky differences in NO2 concentrations over the United States: implications for satellite measurement applications. *Atmos. Chem. Phys.*, *25*(22), 16287-16302. https://doi.org/https://doi.org/10.5194/acp-25-16287-2025
Griffin, D., Zhao, X., McLinden, C., Yazdani, N., Nowlan, C. R., Abad, G. G., Fioletov, V., Galarneau, E., Mihele, C., Wren, S., Su, Y., Fehr, L., & Bourassa, A. (2026). Snow-Covered Insights From Above and Below: High-Frequency Measurement of Nitrogen Dioxide From Space and Ground. *Geophysical Research Letters*, *53*(6), e2025GL118440. https://doi.org/https://doi.org/10.1029/2025GL118440
Guttikunda, S., & KA, N. (2022). Evolution of India's PM2.5 pollution between 1998 and 2020 using global reanalysis fields coupled with satellite observations and fuel consumption patterns. *Environmental Science: Atmospheres*, *2*(6), 1502-1515. https://doi.org/10.1039/d2ea00027j
Hallquist, M., Wenger, J. C., Baltensperger, U., Rudich, Y., Simpson, D., Claeys, M., Dommen, J., Donahue, N. M., George, C., Goldstein, A. H., Hamilton, J. F., Herrmann, H., Hoffmann, T., Iinuma, Y., Jang, M., Jenkin, M. E., Jimenez, J. L., Kiendler-Scharr, A., Maenhaut, W., McFiggans, G., Mentel, T. F., Monod, A., Prévôt, A. S. H., Seinfeld, J. H., Surratt, J. D., Szmigielski, R., & Wildt, J. (2009). The formation, properties and impact of secondary organic aerosol: current and emerging issues. *Atmos. Chem. Phys.*, *9*(14), 5155-5236. https://doi.org/10.5194/acp-9-5155-2009

Harel, M., & Price, C. (2020). Thunderstorm Trends over Africa. *Journal of Climate*, *33*(7), 2741-2755. https://doi.org/https://doi.org/10.1175/JCLI-D-18-0781.1
Hauglustaine, D. A., Balkanski, Y., & Schulz, M. (2014). A global model simulation of present and future nitrate aerosols and their direct radiative forcing of climate. *Atmos. Chem. Phys.*, *14*(20), 11031-11063. https://doi.org/https://doi.org/10.5194/acp-14-11031-2014
HealthEffectsInstitute. (2025). *State Global Air Report* Retrieved 12.07.2026 from https://www.stateofglobalair.org/resources/report/state-global-air-report-2025
Heft-Neal, S., Burney, J., Bendavid, E., & Burke, M. (2018). Robust relationship between air quality and infant mortality in Africa. *Nature*, *559*(7713), 254-258. https://doi.org/https://doi.org/10.1038/s41586-018-0263-3
Hickman, Andela, N., Tsigaridis, K., Galy-Lacaux, C., Ossohou, M., & Bauer, S. E. (2021). Reductions in NO₂ burden over north equatorial Africa from decline in biomass burning in spite of growing fossil fuel use, 2005 to 2017. *Proceedings of the National Academy of Sciences*, *118*(7), e2002579118. https://doi.org/https://doi.org/10.1073/pnas.2002579118
Hickman, Huang, Y., Wu, S., Diru, W., Groffman, P. M., Tully, K. L., & Palm, C. A. (2017). Nonlinear response of nitric oxide fluxes to fertilizer inputs and the impacts of agricultural intensification on tropospheric ozone pollution in Kenya. *Global Change Biology*, *23*(8), 3193-3204. https://doi.org/https://doi.org/10.1111/gcb.13644
Hopke, P. K., Dai, Q., Li, L., & Feng, Y. (2020). Global review of recent source apportionments for airborne particulate matter. *Science of The Total Environment*, *740*, 140091. https://doi.org/https://doi.org/10.1016/j.scitotenv.2020.140091
Hsu, C.-H., Henze, D. K., Mizzi, A. P., Harkins, C., Lyu, C., Cooper, O. R., Schwantes, R. H., He, J., Li, M., Wang, S., Stockwell, C. E., Warneke, C., Rollins, A. W., Waxman, E. M., Zuraski, K., Peischl, J., Kondragunta, S., Li, F., Xu, C., Pierce, R. B., Abad, G. G., Nowlan, C. R., Liu, X., & McDonald, B. C. (2026). Top-Down Estimates of U.S. NOx Emissions Using TEMPO and TROPOMI NO2 Remote Sensing Observations With WRF-Chem/Chem-DART. *Journal of Geophysical Research: Atmospheres*, *131*(2), e2025JD044223. https://doi.org/https://doi.org/10.1029/2025JD044223
Huber, D. E., Kerr, G. H., Nawaz, M. O., Runkel, S., Anenberg, S. C., & Goldberg, D. L. (2026). Global NO2 changes between 2019 and 2024 as observed by TROPOMI in urban areas and emerging hotspots. *Atmos. Chem. Phys.*, *26*(5), 3783-3803. https://doi.org/10.5194/acp-26-3783-2026
Hudman, R. C., Moore, N. E., Mebust, A. K., Martin, R. V., Russell, A. R., Valin, L. C., & Cohen, R. C. (2012). Steps towards a mechanistic model of global soil nitric oxide emissions: implementation and space based-constraints. *Atmos. Chem. Phys.*, *12*(16), 7779-7795. https://doi.org/https://doi.org/10.5194/acp-12-7779-2012
Hussein, T., Li, X., Al-Dulaimi, Q., Daour, S., Atashi, N., Viana, M., Alastuey, A., Sogacheva, L., Arar, S., Al-Hunaiti, A., & Petäjä, T. (2020). Particulate Matter Concentrations in a Middle Eastern City – An Insight to Sand and Dust Storm Episodes. *Aerosol and Air Quality Research*, *20*(12), 2780-2792. https://doi.org/https://doi.org/10.4209/aaqr.2020.05.0195
IPCC. (2023). *Climate Change 2023: Synthesis Report. Contribution of Working Groups I, II and III to the Sixth Assessment Report of the Intergovernmental Panel on Climate Change [Core Writing Team, H. Lee and J. Romero (eds.)]. IPCC, Geneva, Switzerland, pp. 35-115,* . Retrieved 11.07.2026 from https://www.ipcc.ch/report/ar6/syr/
Jacob, D., & Bakwin, P. (1991). Cycling of NOx in tropical forest
canopies. In: J. E. Rogers and W. B. Whitman (ed) Microbial Production and Consumption of Greenhouse gases: Methane,

Nitrogen oxides, and Halomethanes. *Washington DC: American Society for Microbiology.*, pp 237–254.

Jaeglé, L., Martin, R. V., Chance, K., Steinberger, L., Kurosu, T. P., Jacob, D. J., Modi, A. I., Yoboué, V., Sigha-Nkamdjou, L., & Galy-Lacaux, C. (2004). Satellite mapping of rain-induced nitric oxide emissions from soils. *Journal of Geophysical Research: Atmospheres*, *109*(D21). https://doi.org/https://doi.org/10.1029/2004JD004787

Jaeglé, L., Steinberger, L., Martin, R. V., & Chance, K. (2005). Global partitioning of NOx sources using satellite observations: Relative roles of fossil fuel combustion, biomass burning and soil emissions [10.1039/B502128F]. *Faraday Discussions*, *130*(0), 407-423. https://doi.org/https://doi.org/10.1039/B502128F

Jin, X., Yang, Y., Gonzalez Abad, G., Nowlan, C., & Liu, X. (2025). Observing the Diurnal Variations of Ozone-NOx-VOC Chemistry Over the U.S. From the Geostationary TEMPO Instrument. *Geophysical Research Letters*, *52*(14), e2025GL116394. https://doi.org/https://doi.org/10.1029/2025GL116394

Kansakar, P., & Hossain, F. (2016). A review of applications of satellite earth observation data for global societal benefit and stewardship of planet earth. *Space Policy*, *36*, 46-54. https://doi.org/https://doi.org/10.1016/j.spacepol.2016.05.005

Kaplan, W. A., Wofsy, S. C., Keller, M., & Da Costa, J. M. (1988). Emission of NO and deposition of O3 in a tropical forest system. *Journal of Geophysical Research: Atmospheres*, *93*(D2), 1389-1395. https://doi.org/https://doi.org/10.1029/JD093iD02p01389

Karagulian, F., Temimi, M., Ghebreyesus, D., Weston, M., Kondapalli, N. K., Valappil, V. K., Aldababesh, A., Lyapustin, A., Chaouch, N., Al Hammadi, F., & Al Abdooli, A. (2019). Analysis of a severe dust storm and its impact on air quality conditions using WRF-Chem modeling, satellite imagery, and ground observations. *Air Quality, Atmosphere & Health*, *12*(4), 453-470. https://doi.org/10.1007/s11869-019-00674-z

Keita, S., Liousse, C., Assamoi, E.-M., Doumbia, T., N'Datchoh, E. T., Gnamien, S., Elguindi, N., Granier, C., and Yoboué, V.: African anthropogenic emissions inventory for gases and particles from 1990 to 2015, Earth Syst. Sci. Data, 13, 3691–3705, https://doi.org/10.5194/essd-13-3691-2021, 2021

Keppens, A., Di Pede, S., Hubert, D., Lambert, J. C., Veefkind, P., Sneep, M., De Haan, J., ter Linden, M., Leblanc, T., Compernolle, S., Verhoelst, T., Granville, J., Nath, O., Fjæraa, A. M., Boyd, I., Niemeijer, S., Van Malderen, R., Smit, H. G. J., Duflot, V., Godin-Beekmann, S., Johnson, B. J., Steinbrecht, W., Tarasick, D. W., Kollonige, D. E., Stauffer, R. M., Thompson, A. M., Dehn, A., & Zehner, C. (2024). 5 years of Sentinel-5P TROPOMI operational ozone profiling and geophysical validation using ozonesonde and lidar ground-based networks. *Atmos. Meas. Tech.*, *17*(13), 3969-3993. https://doi.org/10.5194/amt-17-3969-2024

Keppens, A., Hubert, D., Granville, J., Nath, O., Lambert, J. C., Wespes, C., Coheur, P. F., Clerbaux, C., Boynard, A., Siddans, R., Latter, B., Kerridge, B., Di Pede, S., Veefkind, P., Cuesta, J., Dufour, G., Heue, K. P., Coldewey-Egbers, M., Loyola, D., Orfanoz-Cheuquelaf, A., Maratt Satheesan, S., Eichmann, K. U., Rozanov, A., Sofieva, V. F., Ziemke, J. R., Inness, A., Van Malderen, R., & Hoffmann, L. (2025). Harmonisation of sixteen tropospheric ozone satellite data records. *Atmos. Meas. Tech.*, *18*(22), 6893-6916. https://doi.org/10.5194/amt-18-6893-2025

Lahoz, W. A., Peuch, V. H., Orphal, J., Attié, J. L., Chance, K., Liu, X., Edwards, D., Elbern, H., Flaud, J. M., Claeyman, M., & Amraoui, L. E. (2012). Monitoring Air Quality from Space: The Case for the Geostationary Platform. *Bulletin of the American Meteorological Society*, *93*(2), 221-233. https://doi.org/https://doi.org/10.1175/BAMS-D-11-00045.1

Lapere, R., Mailler, S., & Menut, L. (2021). The 2017 Mega-Fires in Central Chile: Impacts on Regional Atmospheric Composition and Meteorology Assessed from Satellite Data and Chemistry-Transport Modeling. *Atmosphere*, *12*(3), 344. https://www.mdpi.com/2073-4433/12/3/344

Lee, J., Kim, J., Song, C. H., Ryu, J.-H., Ahn, Y.-H., & Song, C. K. (2010). Algorithm for retrieval of aerosol optical properties over the ocean from the Geostationary Ocean Color Imager. *Remote Sensing of Environment*, *114*(5), 1077-1088. https://doi.org/https://doi.org/10.1016/j.rse.2009.12.021

Lelieveld, J., Beirle, S., Hörmann, C., Stenchikov, G., & Wagner, T. (2015). Abrupt recent trend changes in atmospheric nitrogen dioxide over the Middle East. *Science Advances*, *1*(7), e1500498. https://doi.org/https://doi.org/10.1126/sciadv.1500498

Lelieveld, J., Hoor, P., Jöckel, P., Pozzer, A., Hadjinicolaou, P., Cammas, J. P., & Beirle, S. (2009). Severe ozone air pollution in the Persian Gulf region. *Atmos. Chem. Phys.*, *9*(4), 1393-1406. https://doi.org/https://doi.org/10.5194/acp-9-1393-2009

Levelt, P. F., Stein Zweers, D. C., Aben, I., Bauwens, M., Borsdorff, T., De Smedt, I., Eskes, H. J., Lerot, C., Loyola, D. G., Romahn, F., Stavrakou, T., Theys, N., Van Roozendael, M., Veefkind, J. P., & Verhoelst, T. (2022). Air quality impacts of COVID-19 lockdown measures detected from space using high spatial resolution observations of multiple trace gases from Sentinel-5P/TROPOMI. *Atmos. Chem. Phys.*, *22*(15), 10319-10351. https://doi.org/10.5194/acp-22-10319-2022

Li, Shen, F., & Sun, X. (2021). 2019–2020 Australian bushfire air particulate pollution and impact on the South Pacific Ocean. *Scientific Reports*, *11*(1), 12288. https://doi.org/10.1038/s41598-021-91547-y

Li, Wang, J., Zhang, H., Diner, D. J., Hasheminassab, S., & Janechek, N. (2024). Improvement of Surface PM2.5 Diurnal Variation Simulations in East Africa for the MAIA Satellite Mission. *ACS ES&T Air*, *1*(4), 223-233. https://doi.org/https://doi.org/10.1021/acsestair.3c00008

Li, C., Krotkov, N. A., Joiner, J., Carn, S., Fioletov, V., McLinden, C., Griffin, D., Liu, X., & Chong, H. (2025). Hourly Sulfur Dioxide Observations Over North America: First Retrieval Results From TEMPO. *Geophysical Research Letters*, *52*(14), e2025GL115788. https://doi.org/https://doi.org/10.1029/2025GL115788

Li, S., Song, G., Xing, J., Dong, J., Zhang, M., Fan, C., Meng, S., Yang, J., Dong, L., & Gong, W. (2025). Unraveling overestimated exposure risks through hourly ozone retrievals from next-generation geostationary satellites. Nature Communications, 16, 3364. https://doi.org/10.1038/s41467-025-58652-2

Liang, Z., Gu, D., Zhang, M., Yang, N., Zhao, C., Li, R., Wang, Q., Ye, Y., Liu, J., Li, X., Liu, R., Zhang, Y., & Cao, X. (2024). Diurnal Carbon Monoxide Retrieval from FY-4B/GIIRS Using a Novel Machine Learning Method. *Journal of Remote Sensing*, *4*, 0289. https://doi.org/doi:10.34133/remotesensing.0289

Lin, M., Horowitz, L. W., Xie, Y., & De Smedt, I. (2025). Compound Drivers of Rising Ozone Extremes in the North China Plain (2013–2023): Aerosol Decline, Hot Droughts, Afforestation-Driven BVOCs, and Reduced Vegetation Uptake. *Journal of Geophysical Research: Atmospheres*, *130*(24), e2025JD044764. https://doi.org/https://doi.org/10.1029/2025JD044764

Liousse, C., Assamoi, E., Criqui, P., Granier, C., & Rosset, R. (2014). Explosive growth in African combustion emissions from 2005 to 2030. *Environmental Research Letters*, *9*(3), 035003. https://doi.org/https://doi.org/10.1088/1748-9326/9/3/035003

Liu, Y., Brito, J., Dorris, M. R., Rivera-Rios, J. C., Seco, R., Bates, K. H., Artaxo, P., Duvoisin, S., Keutsch, F. N., Kim, S., Goldstein, A. H., Guenther, A. B., Manzi, A. O., Souza, R. A.

F., Springston, S. R., Watson, T. B., McKinney, K. A., & Martin, S. T. (2016). Isoprene photochemistry over the Amazon rainforest. *Proceedings of the National Academy of Sciences*, *113*(22), 6125-6130. https://doi.org/https://doi.org/10.1073/pnas.1524136113
Lourens, A., Butler, T., Beukes, J., van Zyl, P., Beirle, S., Wagner, T., Heue, K.-P., Pienaar, J., Fourie, G., & Lawrence, M. (2012). Re-evaluating the NO2 hotspot over the South African Highveld. *South African Journal of Science*, *108*(11/12), 6 pages. https://doi.org/https://doi.org/10.4102/sajs.v108i11/12.1146
Malashock, D. A., Delang, M. N., Becker, J. S., Serre, M. L., West, J. J., Chang, K.-L., Cooper, O. R., & Anenberg, S. C. (2022). Global trends in ozone concentration and attributable mortality for urban, peri-urban, and rural areas between 2000 and 2019: a modelling study. *The Lancet Planetary Health*, *6*(12), e958-e967. https://doi.org/10.1016/S2542-5196(22)00260-1
Maleki, H., Sorooshian, A., Alam, K., Fathi, A., Weckwerth, T., Moazed, H., Jamshidi, A., Babaei, A. A., Hamid, V., Soltani, F., & Goudarzi, G. (2022). The impact of meteorological parameters on PM10 and visibility during the Middle Eastern dust storms. *Journal of Environmental Health Science and Engineering*, *20*(1), 495-507. https://doi.org/https://doi.org/10.1007/s40201-022-00795-1
Malings, C., Westervelt, D. M., Hauryliuk, A., Presto, A. A., Grieshop, A., Bittner, A., Beekmann, M., & Subramanian, R. (2020). Application of low-cost fine particulate mass monitors to convert satellite aerosol optical depth to surface concentrations in North America and Africa. *Atmos. Meas. Tech.*, *13*(7), 3873-3892. https://doi.org/https://amt.copernicus.org/articles/13/3873/2020/10.5194/amt-13-3873-2020
Mallet, M. D. (2021). Meteorological normalisation of PM10 using machine learning reveals distinct increases of nearby source emissions in the Australian mining town of Moranbah. *Atmospheric Pollution Research*, *12*(1), 23-35. https://doi.org/https://doi.org/10.1016/j.apr.2020.08.001
Marais, Akker, O., & Wiedinmyer, C. (2022). Greenhouse gas and air pollutant emissions from power barges (powerships). *Environmental Science: Advances*, *1*(2), 164-169. https://doi.org/10.1039/d1va00049g
Marais, Jacob, D. J., Choi, S., Joiner, J., Belmonte-Rivas, M., Cohen, R. C., Beirle, S., Murray, L. T., Schiferl, L. D., Shah, V., & Jaeglé, L. (2018). Nitrogen oxides in the global upper troposphere: interpreting cloud-sliced NO2 observations from the OMI satellite instrument. *Atmos. Chem. Phys.*, *18*(23), 17017-17027. https://doi.org/10.5194/acp-18-17017-2018
Marais, Silvern, R. F., Vodonos, A., Dupin, E., Bockarie, A. S., Mickley, L. J., & Schwartz, J. (2019). Air Quality and Health Impact of Future Fossil Fuel Use for Electricity Generation and Transport in Africa. *Environmental Science & Technology*, *53*(22), 13524-13534. https://doi.org/https://doi.org/10.1021/acs.est.9b04958
Marais, & Wiedinmyer, C. (2016). Air Quality Impact of Diffuse and Inefficient Combustion Emissions in Africa (DICE-Africa). *Environmental Science & Technology*, *50*(19), 10739-10745. https://doi.org/10.1021/acs.est.6b02602
Martin, R. V., Fiore, A. M., & Van Donkelaar, A. (2004). Space-based diagnosis of surface ozone sensitivity to anthropogenic emissions. *Geophysical Research Letters*, *31*(6). https://doi.org/https://doi.org/10.1029/2004GL019416
Metz, E.-M., Vardag, S. N., Basu, S., Jung, M., Ahrens, B., El-Madany, T., Sitch, S., Arora, V. K., Briggs, P. R., Friedlingstein, P., Goll, D. S., Jain, A. K., Kato, E., Lombardozzi, D., Nabel, J. E. M. S., Poulter, B., Séférian, R., Tian, H., Wiltshire, A., Yuan, W., Yue, X., Zaehle, S., Deutscher, N. M., Griffith, D. W. T., & Butz, A. (2023). Soil

respiration–driven CO₂ pulses dominate Australia’s flux variability. *Science*, *379*(6639), 1332-1335. https://doi.org/https://doi.org/10.1126/science.add7833

Millet, D. B., Palmer, P. I., Levelt, P. F., Gallardo, L., & Shikwambana, L. (2024). Coordinated Geostationary, Multispectral Satellite Observations Are Critical for Climate and Air Quality Progress. *AGU Advances*, *5*(5), e2024AV001322. https://doi.org/https://doi.org/10.1029/2024AV001322

Mills, G., Pleijel, H., Malley, C. S., Sinha, B., Cooper, O. R., Schultz, M. G., Neufeld, H. S., Simpson, D., Sharps, K., Feng, Z., Gerosa, G., Harmens, H., Kobayashi, K., Saxena, P., Paoletti, E., Sinha, V., & Xu, X. (2018). Tropospheric Ozone Assessment Report: Present-day tropospheric ozone distribution and trends relevant to vegetation. *Elementa: Science of the Anthropocene*, *6*. https://doi.org/https://doi.org/10.1525/elementa.302

Miyazaki, K., Eskes, H., Sudo, K., Boersma, K. F., Bowman, K., & Kanaya, Y. (2017). Decadal changes in global surface NOx emissions from multi-constituent satellite data assimilation. *Atmos. Chem. Phys.*, *17*(2), 807-837. https://doi.org/https://doi.org/10.5194/acp-17-807-2017

Morton, D. C., DeFries, R. S., Randerson, J. T., Giglio, L., Schroeder, W., & van der Werf, G. R. (2008). Agricultural intensification increases deforestation fire activity in Amazonia. *Global Change Biology*, *14*(10), 2262-2275. https://doi.org/https://doi.org/10.1111/j.1365-2486.2008.01652.x

Naeger, A. R., Newchurch, M. J., Moore, T., Chance, K., Liu, X., Alexander, S., Murphy, K., & Wang, B. (2021). Revolutionary Air-Pollution Applications from Future Tropospheric Emissions: Monitoring of Pollution (TEMPO) Observations. *Bulletin of the American Meteorological Society*, *102*(9), E1735-E1741. https://doi.org/https://doi.org/10.1175/BAMS-D-21-0050.1

Nascimento, J. P., Barbosa, H. M. J., Banducci, A. L., Rizzo, L. V., Vara-Vela, A. L., Meller, B. B., Gomes, H., Cezar, A., Franco, M. A., Ponczek, M., Wolff, S., Bela, M. M., & Artaxo, P. (2022). Major Regional-Scale Production of O3 and Secondary Organic Aerosol in Remote Amazon Regions from the Dynamics and Photochemistry of Urban and Forest Emissions. *Environmental Science & Technology*, *56*(14), 9924-9935. https://doi.org/https://doi.org/10.1021/acs.est.2c01358

Nassar, R., McLinden, C., Sioris, C. E., McElroy, C. T., Mendonca, J., Tamminen, J., MacDonald, C. G., Adams, C., Boisvenue, C., Bourassa, A., Cooney, R., Degenstein, D., Drolet, G., Garand, L., Girard, R., Johnson, M., Jones, D. B. A., Kolonjari, F., Kuwahara, B., Martin, R. V., Miller, C. E., O'Neill, N., Riihelä, A., Roche, S., Sander, S. P., Simpson, W. R., Singh, G., Strong, K., Trishchenko, A. P., van Mierlo, H., Zanjani, Z. V., Walker, K. A., & Wunch, D. (2019). The Atmospheric Imaging Mission for Northern Regions: AIM-North. *Canadian Journal of Remote Sensing*, *45*(3-4), 423-442. https://doi.org/10.1080/07038992.2019.1643707

Nassar R, MacDonald CG, Kuwahara B, Fogal A, Issa J, Girmenia A, Khan S and Sioris CE (2023) Intelligent pointing increases the fraction of cloud-free CO2 and CH4 observations from space. Front. Remote Sens. 4:1233803. doi: 10.3389/frsen.2023.1233803

Nawaz, M. O., Huber, D. E., Kerr, G. H., Judd, L. M., Acker, S. J., & Goldberg, D. L. (2025). A Comparative Analysis of TEMPO NO2 Remote Sensing With Surface-Level Monitoring Through Diurnal and Seasonal Trends, Meteorology, and Monitor Characteristics. *Journal of Geophysical Research: Atmospheres*, *130*(20), e2025JD043923. https://doi.org/https://doi.org/10.1029/2025JD043923

O'Dell, K., Kondragunta, S., Zhang, H., Goldberg, D. L., Kerr, G. H., Wei, Z., Henderson, B. H., & Anenberg, S. C. (2024). Public Health Benefits From Improved Identification of Severe Air Pollution Events With Geostationary Satellite Data. *GeoHealth*, *8*(1), e2023GH000890. https://doi.org/https://doi.org/10.1029/2023GH000890

Occhipinti, L., & Oluwasanya, P. (2017). Particulate matter monitoring: Past, present and future. *International Journal of Earth & Environmental Sciences*, *2*, 4. https://doi.org/https://doi.org/10.15344/2456-351X/2017/144

Oetjen, H., Payne, V. H., Kulawik, S. S., Eldering, A., Worden, J., Edwards, D. P., Francis, G. L., Worden, H. M., Clerbaux, C., Hadji-Lazaro, J., & Hurtmans, D. (2014). Extending the satellite data record of tropospheric ozone profiles from Aura-TES to MetOp-IASI: characterisation of optimal estimation retrievals. *Atmos. Meas. Tech.*, *7*(12), 4223-4236. https://doi.org/10.5194/amt-7-4223-2014

Ortega, I., Hannigan, J. W., Edwards, D., Stremme, W., Grutter, M., Cadena-Caicedo, A., Strong, K., Flood, V., Zhao, X., Gonzalez Abad, G., & Nowlan, C. R. (2026). Evaluating TEMPO Formaldehyde Retrievals With Co-Located Ground-Based FTIR and Pandora Observations. *Journal of Geophysical Research: Atmospheres*, *131*(9), e2026JD046497. https://doi.org/https://doi.org/10.1029/2026JD046497

Ossohou, M., Galy-Lacaux, C., Yoboué, V., Hickman, J. E., Gardrat, E., Adon, M., Darras, S., Laouali, D., Akpo, A., Ouafo, M., Diop, B., & Opepa, C. (2019). Trends and seasonal variability of atmospheric NO2 and HNO3 concentrations across three major African biomes inferred from long-term series of ground-based and satellite measurements. *Atmospheric Environment*, *207*, 148-166. https://doi.org/https://doi.org/10.1016/j.atmosenv.2019.03.027

Pang, J., Liu, Z., Wang, X., Bresch, J., Ban, J., Chen, D., & Kim, J. (2018). Assimilating AOD retrievals from GOCI and VIIRS to forecast surface PM2.5 episodes over Eastern China. *Atmospheric Environment*, *179*, 288-304. https://doi.org/https://doi.org/10.1016/j.atmosenv.2018.02.011

Park, J., Hong, H., Lee, H., Kim, S.-W., Kim, J., Van Roozendael, M., Fayt, C., Ahn, M.-H., Jacob, D. J., Seo, S., Kim, K.-M., Kim, D., Choi, W., Lee, W.-J., Lee, D.-W., Wagner, T., Richter, A., Krotkov, N. A., Lamsal, L. N., Ko, D. H., Lee, S. H., & Woo, J.-H. (2025). Tropospheric nitrogen dioxide levels vary diurnally in Asian cities. *Communications Earth & Environment*, *6*(1), 389. https://doi.org/10.1038/s43247-025-02272-7

Pathak, M., & Kuttippurath, J. (2022). Air quality trends in rural India: analysis of NO2 pollution using satellite measurements. *Environmental Science: Processes & Impacts*, *24*(12), 2437-2449. https://doi.org/10.1039/d2em00293k

Paton-Walsh, C., Emmerson, K. M., Garland, R. M., Keywood, M., Hoelzemann, J. J., Huneeus, N., Buchholz, R. R., Humphries, R. S., Altieri, K., Schmale, J., Wilson, S. R., Labuschagne, C., Kalisa, E., Fisher, J. A., Deutscher, N. M., van Zyl, P. G., Beukes, J. P., Joubert, W., Martin, L., Mkololo, T., Barbosa, C., de Fatima Andrade, M., Schofield, R., Mallet, M. D., Harvey, M. J., Formenti, P., Piketh, S. J., & Olivares, G. (2022). Key challenges for tropospheric chemistry in the Southern Hemisphere. *Elementa: Science of the Anthropocene*, *10*(1). https://doi.org/https://doi.org/10.1525/elementa.2021.00050

Paton-Walsh, C., Rayner, P., Simmons, J., Fiddes, S. L., Schofield, R., Bridgman, H., Beaupark, S., Broome, R., Chambers, S. D., Chang, L. T.-C., Cope, M., Cowie, C. T., Desservettaz, M., Dominick, D., Emmerson, K., Forehead, H., Galbally, I. E., Griffiths, A., Guérette, É.-A., Haynes, A., Heyworth, J., Jalaludin, B., Kan, R., Keywood, M., Monk, K., Morgan, G. G., Nguyen Duc, H., Phillips, F., Popek, R., Scorgie, Y., Silver, J. D., Utembe, S., Wadlow, I., Wilson, S. R., & Zhang, Y. (2019). A Clean Air Plan for

Sydney: An Overview of the Special Issue on Air Quality in New South Wales. *Atmosphere*, *10*(12), 774. https://www.mdpi.com/2073-4433/10/12/774
Payne, V. H., Kulawik, S. S., Fischer, E. V., Brewer, J. F., Huey, L. G., Miyazaki, K., Worden, J. R., Bowman, K. W., Hintsa, E. J., Moore, F., Elkins, J. W., & Juncosa Calahorrano, J. (2022). Satellite measurements of peroxyacetyl nitrate from the Cross-Track Infrared Sounder: comparison with ATom aircraft measurements. *Atmos. Meas. Tech.*, *15*(11), 3497-3511. https://doi.org/10.5194/amt-15-3497-2022
Pennington, E. A., Osterman, G. B., Payne, V. H., Miyazaki, K., Bowman, K. W., & Neu, J. L. (2025). Quantifying biases in TROPESS AIRS, CrIS, and joint AIRS+OMI tropospheric ozone products using ozonesondes. *Atmos. Chem. Phys.*, *25*(15), 8533-8552. https://doi.org/10.5194/acp-25-8533-2025
Petzold, A., Thouret, V., Gerbig, C., Zahn, A., Brenninkmeijer, C. A. M., Gallagher, M., Hermann, M., Pontaud, M., Ziereis, H., Boulanger, D., Marshall, J., Nédélec, P., Smit, H. G. J., Friess, U., Flaud, J.-M., Wahner, A., Cammas, J.-P., Volz-Thomas, A., & Team, I. (2015). Global-scale atmosphere monitoring by in-service aircraft – current achievements and future prospects of the European Research Infrastructure IAGOS. *Tellus B: Chemical and Physical Meteorology*. https://doi.org/10.3402/tellusb.v67.28452
Polonsky, I. N., O'Brien, D. M., Kumer, J. B., O'Dell, C. W., & the geo, C. T. (2014). Performance of a geostationary mission, geoCARB, to measure CO₂, CH₄ and CO column-averaged concentrations. *Atmos. Meas. Tech.*, *7*(4), 959-981. https://doi.org/10.5194/amt-7-959-2014
Pope, R. J., Kerridge, B. J., Siddans, R., Latter, B. G., Chipperfield, M. P., Feng, W., Pimlott, M. A., Dhomse, S. S., Retscher, C., & Rigby, R. (2023). Investigation of spatial and temporal variability in lower tropospheric ozone from RAL Space UV–Vis satellite products. *Atmospheric Chemistry and Physics*, *23*(23), 14933-14947.
Potts, D. A., Ferranti, E. J. S., & Hey, J. D. V. (2024). Investigating the barriers and pathways to implementing satellite data into air quality monitoring, regulation and policy design in the United Kingdom. *Environmental Science & Policy*, *151*, 103621. https://doi.org/https://doi.org/10.1016/j.envsci.2023.103621
Qie, K., Tian, W., Wang, W., Wu, X., Yuan, T., Tian, H., Luo, J., Zhang, R., & Wang, T. (2020). Regional trends of lightning activity in the tropics and subtropics. *Atmospheric Research*, *242*, 104960. https://doi.org/https://doi.org/10.1016/j.atmosres.2020.104960
Qu, Z., Henze, D. K., Cooper, O. R., & Neu, J. L. (2020). Impacts of global NOx inversions on NO2 and ozone simulations. *Atmos. Chem. Phys.*, *20*(21), 13109-13130. https://doi.org/https://doi.org/10.5194/acp-20-13109-2020
Riley, M. L., Jiang, N., Duc, H. N., & Azzi, M. (2023). Long-Term Trends in Inferred Continental Background Ozone in Eastern Australia. *Atmosphere*, *14*(7), 1104. https://www.mdpi.com/2073-4433/14/7/1104
Riley, M. L., Watt, S., & Jiang, N. (2022). Tropospheric ozone measurements at a rural town in New South Wales, Australia. *Atmospheric Environment*, *281*, 119143. https://doi.org/https://doi.org/10.1016/j.atmosenv.2022.119143
Rocha, F. O. d., Barbosa, J. L., Campos, V. P., & Alves, R. S. (2022). Nitrogen oxides levels in the atmosphere of different Brazilian urban centers, by passive sampling. *Journal of the Brazilian Chemical Society*, *33*(2), 143-156. https://doi.org/https://doi.org/10.21577/0103-5053.20210131
Rumpff, L., Legge, S. M., Van Leeuwen, S., Wintle, B. A., & Woinarski, J. C. (2023). *Australia's megafires: Biodiversity impacts and lessons from 2019-2020*. CSIRO Publishing. https://doi.org/https://ebooks.publish.csiro.au/content/australias-megafires

Ryan, Rhodes, S., Tully, M., Wilson, S., Jones, N., Frieß, U., & Schofield, R. (2018). Daytime HONO, NO2 and aerosol distributions from MAX-DOAS observations in Melbourne. *Atmos. Chem. Phys.*, *18*(19), 13969-13985. https://doi.org/10.5194/acp-18-13969-2018

Ryan, R. G., Silver, J. D., & Schofield, R. (2021). Air quality and health impact of 2019–20 Black Summer megafires and COVID-19 lockdown in Melbourne and Sydney, Australia. *Environmental Pollution*, *274*, 116498. https://doi.org/https://doi.org/10.1016/j.envpol.2021.116498

Saide, P. E., Kim, J., Song, C. H., Choi, M., Cheng, Y., & Carmichael, G. R. (2014). Assimilation of next generation geostationary aerosol optical depth retrievals to improve air quality simulations. *Geophysical Research Letters*, *41*(24), 9188-9196. https://doi.org/https://doi.org/10.1002/2014GL062089

Saunois, M., Reeves, C. E., Mari, C. H., Murphy, J. G., Stewart, D. J., Mills, G. P., Oram, D. E., & Purvis, R. M. (2009). Factors controlling the distribution of ozone in the West African lower troposphere during the AMMA (African Monsoon Multidisciplinary Analysis) wet season campaign. *Atmos. Chem. Phys.*, *9*(16), 6135-6155. https://doi.org/https://doi.org/10.5194/acp-9-6135-2009

Sauvage, B., Thouret, V., Cammas, J. P., Gheusi, F., Athier, G., & Nédélec, P. (2005). Tropospheric ozone over Equatorial Africa: regional aspects from the MOZAIC data. *Atmos. Chem. Phys.*, *5*(2), 311-335. https://doi.org/10.5194/acp-5-311-2005

Schneider, P., Lahoz, W. A., & van der A, R. (2015). Recent satellite-based trends of tropospheric nitrogen dioxide over large urban agglomerations worldwide. *Atmos. Chem. Phys.*, *15*(3), 1205-1220. https://doi.org/10.5194/acp-15-1205-2015

Schneider, P., & van der A, R. J. (2012). A global single-sensor analysis of 2002–2011 tropospheric nitrogen dioxide trends observed from space. *Journal of Geophysical Research: Atmospheres*, *117*(D16). https://doi.org/https://doi.org/10.1029/2012JD017571

Schröder, S., Schultz, M. G., Selke, N., Sun, J., Ahring, J., Mozaffari, A., Romberg, M., Epp, E., Lensing, M., & Apweiler, S. (2021). TOAR data infrastructure. *FZ-Juelich*. https://doi.org/https://doi.org/10.34730/4D9A287DEC0B42F1AA6D244DE8F19EB3

Schultz, M. G., Schröder, S., Lyapina, O., Cooper, O. R., Galbally, I., Petropavlovskikh, I., von Schneidemesser, E., Tanimoto, H., Elshorbany, Y., Naja, M., Seguel, R. J., Dauert, U., Eckhardt, P., Feigenspan, S., Fiebig, M., Hjellbrekke, A.-G., Hong, Y.-D., Kjeld, P. C., Koide, H., Lear, G., Tarasick, D., Ueno, M., Wallasch, M., Baumgardner, D., Chuang, M.-T., Gillett, R., Lee, M., Molloy, S., Moolla, R., Wang, T., Sharps, K., Adame, J. A., Ancellet, G., Apadula, F., Artaxo, P., Barlasina, M. E., Bogucka, M., Bonasoni, P., Chang, L., Colomb, A., Cuevas-Agulló, E., Cupeiro, M., Degorska, A., Ding, A., Fröhlich, M., Frolova, M., Gadhavi, H., Gheusi, F., Gilge, S., Gonzalez, M. Y., Gros, V., Hamad, S. H., Helmig, D., Henriques, D., Hermansen, O., Holla, R., Hueber, J., Im, U., Jaffe, D. A., Komala, N., Kubistin, D., Lam, K.-S., Laurila, T., Lee, H., Levy, I., Mazzoleni, C., Mazzoleni, L. R., McClure-Begley, A., Mohamad, M., Murovec, M., Navarro-Comas, M., Nicodim, F., Parrish, D., Read, K. A., Reid, N., Ries, L., Saxena, P., Schwab, J. J., Scorgie, Y., Senik, I., Simmonds, P., Sinha, V., Skorokhod, A. I., Spain, G., Spangl, W., Spoor, R., Springston, S. R., Steer, K., Steinbacher, M., Suharguniyawan, E., Torre, P., Trickl, T., Weili, L., Weller, R., Xiaobin, X., Xue, L., & Zhiqiang, M. (2017). Tropospheric Ozone Assessment Report: Database and metrics data of global surface ozone observations. *Elementa: Science of the Anthropocene*, *5*. https://doi.org/10.1525/elementa.244

Science. (2026). *With new environmental law, China expands its 'war on pollution'*. Retrieved 11.07.2026 from https://www.science.org/content/article/new-environmental-law-china-expands-its-war-pollution

Seguel, R. J., Castillo, L., Opazo, C., Rojas, N. Y., Nogueira, T., Cazorla, M., Gavidia-Calderón, M., Gallardo, L., Garreaud, R., Carrasco-Escaff, T., & Elshorbany, Y. (2024). Changes in South American surface ozone trends: exploring the influences of precursors and extreme events. *Atmos. Chem. Phys.*, *24*(14), 8225-8242. https://doi.org/10.5194/acp-24-8225-2024

Seinfeld, J. H., & Pandis, S. N. (2016). *Atmospheric chemistry and physics: from air pollution to climate change*. John Wiley & Sons.

Shaddick, G., Thomas, M. L., Mudu, P., Ruggeri, G., & Gumy, S. (2020). Half the world's population are exposed to increasing air pollution. *npj Climate and Atmospheric Science*, *3*(1), 23. https://doi.org/10.1038/s41612-020-0124-2

Shahid, I., Shahzad, M. I., Tutsak, E., Mahfouz, M. M. K., Al Adba, M. S., Abbasi, S. A., Rathore, H. A., Asif, Z., & Chen, Z. (2024). Carbon based sensors for air quality monitoring networks; middle east perspective [Review]. *Frontiers in Chemistry*, *Volume 12 - 2024*. https://doi.org/https://doi.org/10.3389/fchem.2024.1391409

Sheng, M., Zhou, R., Hua, J., Han, S., Zhang, L., Wang, W., Dang, R., Cao, H., Chen, Z., Gu, Y., Liu, M., Lee, L., Qi, C., Han, C., Shephard, M. W., Guendouz, N., Viatte, C., Clarisse, L., Van Damme, M., Clerbaux, C., & Zeng, Z. C. (2025). Geostationary observations of atmospheric ammonia over East Asia: spatio-temporal variations revealed by three years of FY-4B/GIIRS measurements. *EGUsphere*, *2025*, 1-36. https://doi.org/https://doi.org/10.5194/egusphere-2025-5699

Shrivastava, M., Andreae, M. O., Artaxo, P., Barbosa, H. M. J., Berg, L. K., Brito, J., Ching, J., Easter, R. C., Fan, J., Fast, J. D., Feng, Z., Fuentes, J. D., Glasius, M., Goldstein, A. H., Alves, E. G., Gomes, H., Gu, D., Guenther, A., Jathar, S. H., Kim, S., Liu, Y., Lou, S., Martin, S. T., McNeill, V. F., Medeiros, A., de Sá, S. S., Shilling, J. E., Springston, S. R., Souza, R. A. F., Thornton, J. A., Isaacman-VanWertz, G., Yee, L. D., Ynoue, R., Zaveri, R. A., Zelenyuk, A., & Zhao, C. (2019). Urban pollution greatly enhances formation of natural aerosols over the Amazon rainforest. *Nature Communications*, *10*(1), 1046. https://doi.org/https://doi.org/10.1038/s41467-019-08909-4

Shrivastava, M., Cappa, C. D., Fan, J., Goldstein, A. H., Guenther, A. B., Jimenez, J. L., Kuang, C., Laskin, A., Martin, S. T., Ng, N. L., Petaja, T., Pierce, J. R., Rasch, P. J., Roldin, P., Seinfeld, J. H., Shilling, J., Smith, J. N., Thornton, J. A., Volkamer, R., Wang, J., Worsnop, D. R., Zaveri, R. A., Zelenyuk, A., & Zhang, Q. (2017). Recent advances in understanding secondary organic aerosol: Implications for global climate forcing. *Reviews of Geophysics*, *55*(2), 509-559. https://doi.org/https://doi.org/10.1002/2016RG000540

Shu, L., Zhu, L., Bak, J., Zoogman, P., Han, H., Liu, S., Li, X., Sun, S., Li, J., Chen, Y., Pu, D., Zuo, X., Fu, W., Yang, X., & Fu, T. M. (2023). Improving ozone simulations in Asia via multisource data assimilation: results from an observing system simulation experiment with GEMS geostationary satellite observations. *Atmos. Chem. Phys.*, *23*(6), 3731-3748. https://doi.org/10.5194/acp-23-3731-2023

Sicard, P., Agathokleous, E., Anenberg, S. C., De Marco, A., Paoletti, E., & Calatayud, V. (2023). Trends in urban air pollution over the last two decades: A global perspective. *Science of The Total Environment*, *858*, 160064. https://doi.org/https://doi.org/10.1016/j.scitotenv.2022.160064

Singh, N., Dey, S., & Knibbs, L. D. (2023). Spatio-temporal patterns of tropospheric NO2 over India during 2005–2019. *Atmospheric Pollution Research*, *14*(3), 101692. https://doi.org/https://doi.org/10.1016/j.apr.2023.101692

Siu, T. K., Goldberg, D. L., Kerr, G. H., Chen, L., Nawaz, M. O., Chang, R. Y.-W., & Fong, K. C. (2025). Tropospheric NO2 Patterns in Eastern Canada Using the First Year of TEMPO

Observations. *Journal of Geophysical Research: Atmospheres*, *130*(24), e2025JD044757. https://doi.org/https://doi.org/10.1029/2025JD044757

Snider, G., Weagle, C. L., Martin, R. V., van Donkelaar, A., Conrad, K., Cunningham, D., Gordon, C., Zwicker, M., Akoshile, C., Artaxo, P., Anh, N. X., Brook, J., Dong, J., Garland, R. M., Greenwald, R., Griffith, D., He, K., Holben, B. N., Kahn, R., Koren, I., Lagrosas, N., Lestari, P., Ma, Z., Vanderlei Martins, J., Quel, E. J., Rudich, Y., Salam, A., Tripathi, S. N., Yu, C., Zhang, Q., Zhang, Y., Brauer, M., Cohen, A., Gibson, M. D., & Liu, Y. (2015). SPARTAN: a global network to evaluate and enhance satellite-based estimates of ground-level particulate matter for global health applications. *Atmos. Meas. Tech.*, *8*(1), 505-521. https://doi.org/10.5194/amt-8-505-2015

Souri, A. H., Nowlan, C. R., Wolfe, G. M., Lamsal, L. N., Chan Miller, C. E., Abad, G. G., Janz, S. J., Fried, A., Blake, D. R., Weinheimer, A. J., Diskin, G. S., Liu, X., & Chance, K. (2020). Revisiting the effectiveness of HCHO/NO2 ratios for inferring ozone sensitivity to its precursors using high resolution airborne remote sensing observations in a high ozone episode during the KORUS-AQ campaign. *Atmospheric Environment*, *224*, 117341. https://doi.org/https://doi.org/10.1016/j.atmosenv.2020.117341

Streets, D. G., Canty, T., Carmichael, G. R., de Foy, B., Dickerson, R. R., Duncan, B. N., Edwards, D. P., Haynes, J. A., Henze, D. K., Houyoux, M. R., Jacob, D. J., Krotkov, N. A., Lamsal, L. N., Liu, Y., Lu, Z., Martin, R. V., Pfister, G. G., Pinder, R. W., Salawitch, R. J., & Wecht, K. J. (2013). Emissions estimation from satellite retrievals: A review of current capability. *Atmospheric Environment*, *77*, 1011-1042. https://doi.org/https://doi.org/10.1016/j.atmosenv.2013.05.051

Sun, K., Saju, J. A., Nowlan, C. R., González Abad, G., & Liu, X. (2025). Hourly Nitrogen Oxides Emissions Estimated From TEMPO and Comparison With Facility-Level Monitoring Data. *Journal of Geophysical Research: Atmospheres*, *130*(23), e2025JD044565. https://doi.org/https://doi.org/10.1029/2025JD044565

Tarasick, D., Galbally, I. E., Cooper, O. R., Schultz, M. G., Ancellet, G., Leblanc, T., Wallington, T. J., Ziemke, J., Liu, X., Steinbacher, M., Staehelin, J., Vigouroux, C., Hannigan, J. W., García, O., Foret, G., Zanis, P., Weatherhead, E., Petropavlovskikh, I., Worden, H., Osman, M., Liu, J., Chang, K.-L., Gaudel, A., Lin, M., Granados-Muñoz, M., Thompson, A. M., Oltmans, S. J., Cuesta, J., Dufour, G., Thouret, V., Hassler, B., Trickl, T., & Neu, J. L. (2019). Tropospheric Ozone Assessment Report: Tropospheric ozone from 1877 to 2016, observed levels, trends and uncertainties. *Elementa: Science of the Anthropocene*, *7*. https://doi.org/10.1525/elementa.376

Tocquer, F., Barret, B., Mari, C., Le Flochmoën, E., Cammas, J. p., & Sauvage, B. (2015). An upper tropospheric 'ozone river' from Africa to India during the 2008 Asian post-monsoon season. *Tellus B: Chemical and Physical Meteorology*. https://doi.org/https://doi.org/10.3402/tellusb.v67.25350

Torres, A. L., & Buchan, H. (1988). Tropospheric nitric oxide measurements over the Amazon Basin. *Journal of Geophysical Research: Atmospheres*, *93*(D2), 1396-1406. https://doi.org/https://doi.org/10.1029/JD093iD02p01396

Trichtchenko, L. D., Nikitina, L. V., Trishchenko, A. P., & Garand, L. (2014). Highly Elliptical Orbits for Arctic observations: Assessment of ionizing radiation. *Advances in Space Research*, *54*(11), 2398-2414. https://doi.org/https://doi.org/10.1016/j.asr.2014.09.012

Tripathi, N., Krumm, B. E., Edtbauer, A., Ringsdorf, A., Wang, N., Kohl, M., Vella, R., Machado, L. A. T., Pozzer, A., Lelieveld, J., & Williams, J. (2025). Impacts of convection, chemistry, and forest clearing on biogenic volatile organic compounds over the Amazon. *Nature Communications*, *16*(1), 4692. https://doi.org/https://doi.org/10.1038/s41467-025-59953-2

Utembe, S. R., Rayner, P. J., Silver, J. D., Guérette, E.-A., Fisher, J. A., Emmerson, K. M., Cope, M., Paton-Walsh, C., Griffiths, A. D., Duc, H., Monk, K., & Scorgie, Y. (2018). Hot Summers: Effect of Extreme Temperatures on Ozone in Sydney, Australia. *Atmosphere*, *9*(12), 466. https://www.mdpi.com/2073-4433/9/12/466

Vakkari, V., Beukes, J. P., Dal Maso, M., Aurela, M., Josipovic, M., & van Zyl, P. G. (2018). Major secondary aerosol formation in southern African open biomass burning plumes. *Nature Geoscience*, *11*(8), 580-583. https://doi.org/10.1038/s41561-018-0170-0

van der Werf, G. R., Randerson, J. T., Giglio, L., Collatz, G. J., Mu, M., Kasibhatla, P. S., Morton, D. C., DeFries, R. S., Jin, Y., & van Leeuwen, T. T. (2010). Global fire emissions and the contribution of deforestation, savanna, forest, agricultural, and peat fires (1997–2009). *Atmos. Chem. Phys.*, *10*(23), 11707-11735. https://doi.org/https://doi.org/10.5194/acp-10-11707-2010

Vargas, C., Whelan, J., Brimblecombe, J., & Allender, S. (2022). Co-creation, co-design, co-production for public health – a perspective on definitions and distinctions. *Public Health Research & Practice*, *32*(2). https://doi.org/https://doi.org/10.17061/phrp3222211

Verchot, L. V., Davidson, E. A., Cattânio, J. H., & Ackerman, I. L. (2000). Land-Use Change and Biogeochemical Controls of Methane Fluxes in Soils of Eastern Amazonia. *Ecosystems*, *3*(1), 41-56. https://doi.org/https://doi.org/10.1007/s100210000009

Vinken, G. C. M., Boersma, K. F., Maasakkers, J. D., Adon, M., & Martin, R. V. (2014). Worldwide biogenic soil NO_x emissions inferred from OMI NO₂ observations. *Atmos. Chem. Phys.*, *14*(18), 10363-10381. https://doi.org/https://doi.org/10.5194/acp-14-10363-2014

Vohra, K., Madhumitha, S., Chakraborty, A., Shah, H., As, B., & Pakki, J. (2025). Urgent issues regarding real-time air quality monitoring data in India: Unveiling solutions and implications for policy and health. *Atmospheric Environment: X*, *25*, 100308. https://doi.org/https://doi.org/10.1016/j.aeaoa.2024.100308

Vohra, K., Marais, E. A., Bloss, W. J., Schwartz, J., Mickley, L. J., Van Damme, M., Clarisse, L., & Coheur, P.-F. (2022). Rapid rise in premature mortality due to anthropogenic air pollution in fast-growing tropical cities from 2005 to 2018. *Science Advances*, *8*(14), eabm4435. https://doi.org/https://doi.org/10.1126/sciadv.abm4435

Vohra, K., Marais, E. A., Suckra, S., Kramer, L., Bloss, W. J., Sahu, R., Gaur, A., Tripathi, S. N., Van Damme, M., Clarisse, L., & Coheur, P. F. (2021). Long-term trends in air quality in major cities in the UK and India: a view from space. *Atmos. Chem. Phys.*, *21*(8), 6275-6296. https://doi.org/10.5194/acp-21-6275-2021

Wan, N., Xiong, X., Kluitenberg, G. J., Hutchinson, J. M. S., Aiken, R., Zhao, H., & Lin, X. (2023). Estimation of biomass burning emission of NO2 and CO from 2019–2020 Australia fires based on satellite observations. *Atmos. Chem. Phys.*, *23*(1), 711-724. https://doi.org/https://doi.org/10.5194/acp-23-711-2023

Weagle, C. L., Snider, G., Li, C., van Donkelaar, A., Philip, S., Bissonnette, P., Burke, J., Jackson, J., Latimer, R., Stone, E., Abboud, I., Akoshile, C., Anh, N. X., Brook, J. R., Cohen, A., Dong, J., Gibson, M. D., Griffith, D., He, K. B., Holben, B. N., Kahn, R., Keller, C. A., Kim, J. S., Lagrosas, N., Lestari, P., Khian, Y. L., Liu, Y., Marais, E. A., Martins, J. V., Misra, A., Muliane, U., Pratiwi, R., Quel, E. J., Salam, A., Segev, L., Tripathi, S. N., Wang, C., Zhang, Q., Brauer, M., Rudich, Y., & Martin, R. V. (2018). Global Sources of Fine Particulate Matter: Interpretation of PM2.5 Chemical Composition Observed by SPARTAN using a Global Chemical Transport Model. *Environmental Science & Technology*, *52*(20), 11670-11681. https://doi.org/10.1021/acs.est.8b01658

Wei, D., Fuentes, J. D., Gerken, T., Trowbridge, A. M., Stoy, P. C., & Chamecki, M. (2019). Influences of nitrogen oxides and isoprene on ozone-temperature relationships in the Amazon rain forest. *Atmospheric Environment*, *206*, 280-292. https://doi.org/https://doi.org/10.1016/j.atmosenv.2019.02.044

Wells, K. C., Millet, D. B., Brewer, J. F., Payne, V. H., Cady-Pereira, K. E., Pernak, R., Kulawik, S., Vigouroux, C., Jones, N., Mahieu, E., Makarova, M., Nagahama, T., Ortega, I., Palm, M., Strong, K., Schneider, M., Smale, D., Sussmann, R., & Zhou, M. (2025). Global decadal measurements of methanol, ethene, ethyne, and HCN from the Cross-track Infrared Sounder. *Atmos. Meas. Tech.*, *18*(3), 695-716. https://doi.org/10.5194/amt-18-695-2025

Wells, K. C., Millet, D. B., Payne, V. H., Deventer, M. J., Bates, K. H., de Gouw, J. A., Graus, M., Warneke, C., Wisthaler, A., & Fuentes, J. D. (2020). Satellite isoprene retrievals constrain emissions and atmospheric oxidation. *Nature*, *585*(7824), 225-233. https://doi.org/10.1038/s41586-020-2664-3

Whitburn, S., Van Damme, M., Clarisse, L., Bauduin, S., Heald, C. L., Hadji-Lazaro, J., Hurtmans, D., Zondlo, M. A., Clerbaux, C., & Coheur, P.-F. (2016). A flexible and robust neural network IASI-NH3 retrieval algorithm. *Journal of Geophysical Research: Atmospheres*, *121*(11), 6581-6599. https://doi.org/https://doi.org/10.1002/2016JD024828

WHO. (2023). *WHO ambient air quality database, 2022 update: status report*. World Health Organization.

WHO. (2026). *State of the Global Climate 2025 report*. Retrieved 12.07.2026 from https://library.wmo.int/idurl/4/69807

WMO. (2019). Vision for the WMO Integrated Global Observing System in 2040, World Meteorological Organization publication WMO-No. 1243, https://library.wmo.int/idurl/4/57028.

Worden, H. M., Deeter, M. N., Edwards, D. P., Gille, J. C., Drummond, J. R., & Nédélec, P. (2010). Observations of near-surface carbon monoxide from space using MOPITT multispectral retrievals. *Journal of Geophysical Research: Atmospheres*, *115*(D18). https://doi.org/https://doi.org/10.1029/2010JD014242

Yang, Jacob, D. J., Dang, R., Oak, Y. J., Lin, H., Kim, J., Zhai, S., Colombi, N. K., Pendergrass, D. C., Beaudry, E., Shah, V., Feng, X., Yantosca, R. M., Chong, H., Park, J., Lee, H., Lee, W. J., Kim, S., Kim, E., Travis, K. R., Crawford, J. H., & Liao, H. (2024). Interpreting Geostationary Environment Monitoring Spectrometer (GEMS) geostationary satellite observations of the diurnal variation in nitrogen dioxide (NO2) over East Asia. *Atmos. Chem. Phys.*, *24*(12), 7027-7039. https://doi.org/10.5194/acp-24-7027-2024

Yang, Zhao, C., Yang, Y., & Fan, H. (2021). Long-term multi-source data analysis about the characteristics of aerosol optical properties and types over Australia. *Atmos. Chem. Phys.*, *21*(5), 3803-3825. https://doi.org/10.5194/acp-21-3803-2021

Zeng, Z.-C., Franco, B., Clarisse, L., Lee, L., Qi, C., & Lu, F. (2024). Observing a Volatile Organic Compound From a Geostationary Infrared Sounder: HCOOH From FengYun-4B/GIIRS. *Journal of Geophysical Research: Atmospheres*, *129*(19), e2024JD041352. https://doi.org/https://doi.org/10.1029/2024JD041352

Zhang, H., Kondragunta, S., & Ciren, P. (2025). TEMPO Aerosol Optical Depth and Aerosol Layer Height Retrieval Algorithm. *Journal of Geophysical Research: Atmospheres*, *130*(18), e2025JD044082. https://doi.org/https://doi.org/10.1029/2025JD044082

Zhang, H., Wei, Z., Henderson, B. H., Anenberg, S. C., Katelyn, O. D., & Kondragunta, S. (2022). Nowcasting Applications of Geostationary Satellite Hourly Surface PM2.5 Data. *Weather and Forecasting*, *37*(12), 2313-2329. https://doi.org/https://doi.org/10.1175/WAF-D-22-0114.1

Ziemke, J. R., Chandra, S., Labow, G. J., Bhartia, P. K., Froidevaux, L., & Witte, J. C. (2011). A global climatology of tropospheric and stratospheric ozone derived from Aura OMI and MLS measurements. *Atmos. Chem. Phys.*, *11*(17), 9237-9251. https://doi.org/10.5194/acp-11-9237-2011

Ziemke, J. R., Oman, L. D., Strode, S. A., Douglass, A. R., Olsen, M. A., McPeters, R. D., Bhartia, P. K., Froidevaux, L., Labow, G. J., Witte, J. C., Thompson, A. M., Haffner, D. P., Kramarova, N. A., Frith, S. M., Huang, L. K., Jaross, G. R., Seftor, C. J., Deland, M. T., & Taylor, S. L. (2019). Trends in global tropospheric ozone inferred from a composite record of TOMS/OMI/MLS/OMPS satellite measurements and the MERRA-2 GMI simulation. *Atmos. Chem. Phys.*, *19*(5), 3257-3269. https://doi.org/10.5194/acp-19-3257-2019

Zoogman, P., Liu, X., Suleiman, R. M., Pennington, W. F., Flittner, D. E., Al-Saadi, J. A., Hilton, B. B., Nicks, D. K., Newchurch, M. J., Carr, J. L., Janz, S. J., Andraschko, M. R., Arola, A., Baker, B. D., Canova, B. P., Chan Miller, C., Cohen, R. C., Davis, J. E., Dussault, M. E., Edwards, D. P., Fishman, J., Ghulam, A., González Abad, G., Grutter, M., Herman, J. R., Houck, J., Jacob, D. J., Joiner, J., Kerridge, B. J., Kim, J., Krotkov, N. A., Lamsal, L., Li, C., Lindfors, A., Martin, R. V., McElroy, C. T., McLinden, C., Natraj, V., Neil, D. O., Nowlan, C. R., O′Sullivan, E. J., Palmer, P. I., Pierce, R. B., Pippin, M. R., Saiz-Lopez, A., Spurr, R. J. D., Szykman, J. J., Torres, O., Veefkind, J. P., Veihelmann, B., Wang, H., Wang, J., & Chance, K. (2017). Tropospheric emissions: Monitoring of pollution (TEMPO). *Journal of Quantitative Spectroscopy and Radiative Transfer*, *186*, 17-39. https://doi.org/https://doi.org/10.1016/j.jqsrt.2016.05.008

Zubkova, M., Boschetti, L., Abatzoglou, J. T., & Giglio, L. (2019). Changes in Fire Activity in Africa from 2002 to 2016 and Their Potential Drivers. *Geophysical Research Letters*, *46*(13), 7643-7653. https://doi.org/https://doi.org/10.1029/2019GL083469

20. Acronyms

21. Appendix